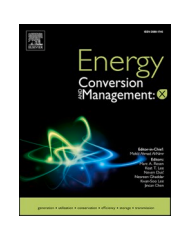
FISEVIER

Contents lists available at ScienceDirect

# Energy Conversion and Management: X

journal homepage: www.sciencedirect.com/journal/energy-conversion-and-management-x





# Novel techno-economic feasibility study of an off-grid PV/wind/diesel/battery hybrid energy system using MATLAB-HOMER link

Saleh Awadh AL Dawsari a, Fatih Anayi a, Michael Packianather

- a School of Engineering, Cardiff University, Cardiff CF24 3AA, UK
- <sup>b</sup> Electrical Engineering Department, College of Engineering, Najran University, Najran, Saudi Arabia

ARTICLE INFO

Keywords: MATLAB-HOMER link Hybrid energy system Off grid microgrid

#### ABSTRACT

This paper investigates the design and optimization of an off-grid hybrid renewable energy system (HRES) for remote areas, combining solar PV, wind turbines, diesel generators, and battery storage. The system is analyzed using a proposed HOMER Pro with a MATLAB-linked dispatch strategy to evaluate technical feasibility and cost-effectiveness under varying weather conditions. A case study in Sharurah, Saudi Arabia, demonstrates the optimal configuration, which includes 5.8 MW of solar PV, 3.2 MW of wind turbines, 4 MWh of battery storage, and 2 MW of diesel backup. The proposed system achieves 100 % renewable energy penetration under optimal conditions, covering 328 % of the annual load demand (14,500 MWh) while generating 41 % excess electricity. Economically, the system yields a Net Present Cost (NPC) of \$16.4 million, eliminating fuel costs and reducing CO<sub>2</sub> emissions by 1200 tons/year. Reliability is ensured with less than 0.1 % unmet load, making it a viable solution for sustainable energy supply in isolated regions. The results highlight the system's ability to balance cost, reliability, and environmental benefits, proving its suitability for off-grid applications.

# 1. Introduction

In recent years, the global demand for reliable and sustainable energy solutions has surged, driven by the growing awareness of the environmental and economic drawbacks of traditional fossil fuel-based energy systems [1]. This shift is particularly pronounced in remote and rural areas, where extending conventional power grids is often prohibitively expensive and technically challenging. As a result, Off-Grid Power Systems (OFFGPS) powered by Renewable Energy Sources (RES) have emerged as a compelling alternative, providing a viable solution to the energy access gap in these regions [2]. This trend extends beyond developing nations, gaining momentum in developed countries as well, where the focus has increasingly turned to reducing carbon footprints and enhancing energy security [3,4].

Driven by urgent climate action and policy support, global renewable energy capacity continued to expand rapidly [5]. By the end of 2023, the total installed renewable capacity reached approximately 3,372 GW, led by solar, wind, hydropower, and biomass. In 2024, a record 700 GW of new renewable capacity was added—marking the 22nd consecutive year of growth—of which 80 % came from solar PV. Global renewable electricity generation increased by over 670 TWh in 2024, accounting for 32 % of total power generation [6]. Renewables,

together with nuclear, provided 80 % of the annual increase in global electricity supply. This reflects a structural shift away from fossil fuels, as oil's share of total energy demand fell below 30 % for the first time since records began. China and the United States remained the largest contributors to renewable capacity expansion. China added the most in absolute terms and now approaches 760 GW of installed renewable capacity. The United States exceeded 265 GW, driven by increased solar and wind integration and the expansion of electric vehicle infrastructure. Africa reached 221 GW, primarily through hydropower, solar PV, and biomass. Looking ahead, global renewable electricity generation is expected to reach over 17,000 TWh by 2030, nearly doubling from 2023 levels. Renewables are set to overtake coal in electricity generation in 2025. Solar PV will become the largest single renewable power source by 2029, surpassing hydropower. These developments are essential for meeting rising electricity demand—driven by extreme temperatures, digitalization, and electric mobility—while limiting global temperature rise to below 1.5  $^{\circ}$ C.

The implementation of OFFGPS in remote areas is fueled by several factors, including the declining costs of photovoltaic (PV) systems, wind turbines, and micro-hydropower, alongside significant advancements in energy storage technologies such as batteries [7,8]. These technological developments have made the deployment of OFFGPS feasible for both

E-mail addresses: Aldawsarisa@cardiff.ac.uk (S.A. AL Dawsari), anayi@cardiff.ac.uk (F. Anayi), packianatherms@cardiff.ac.uk (M. Packianather).

residential and industrial applications, particularly in regions where geographical isolation renders grid extension impractical or economically unviable [9,10]. Saudi Arabia stands out as a unique case study for the implementation of hybrid renewable energy systems due to its abundant solar and wind resources and the government's commitment to diversifying the national energy mix under the Vision 2030 initiative [11].

Despite the substantial potential of RES, their intermittent and variable nature presents challenges to ensuring a reliable power supply. To mitigate these challenges, hybrid renewable energy systems (HRES), which integrate multiple RES with conventional power sources such as diesel generators, have been considered as a main point of research in many studies [12]. HRES offer a more reliable and continuous power supply by harnessing the complementary characteristics of different energy sources. For example, solar power can be utilized during the day, while wind energy can supplement power generation during the night or on overcast days. The integration of energy storage systems further enhances the reliability and stability of HRES, making them particularly suitable for remote and off-grid applications [13,14].

In Saudi Arabia, the relevance of HRES is underscored by the country's vast desert landscapes, characterized by high solar irradiance and significant wind potential [15]. The Vision 2030 plan highlights the importance of diversifying the energy sector and reducing reliance on oil, with an ambitious target of generating 50 % of the country's electricity from renewable sources by 2030 [16]. This target has catalyzed numerous research initiatives and pilot projects focused on the feasibility and optimization of HRES across various regions of the country. A notable case study investigates a remote village in the Al-Jouf region, where the local population has historically depended on diesel generators for electricity. The high cost of diesel fuel and the logistical challenges of fuel transportation underscore the urgency of exploring alternative energy solutions. This study evaluates the feasibility of implementing a hybrid solar-wind-diesel-battery system to meet the village's energy demands [17].

#### 1.1. Literature review

HOMER software is a well-established tool for designing and optimizing hybrid power systems; the paper simulates various scenarios to identify the most cost-effective and reliable configuration [18]. The results demonstrate that the hybrid system not only reduces the levelized cost of electricity (LCOE) but also significantly lowers greenhouse gas emissions compared to the existing diesel-only setup. The optimized configuration includes a combination of solar PV panels, wind turbines, and a diesel generator, supported by a battery storage system to ensure a continuous power supply [19]. The system is designed to operate autonomously with minimal maintenance requirements, making it an ideal solution for remote locations [20]. Furthermore, the inclusion of energy storage addresses the intermittency of solar and wind power, ensuring consistent electricity supply throughout the year [21]. The study highlights the importance of considering local climatic conditions, resource availability, and load profiles when designing HRES. In the Saudi Arabian context, the high solar potential makes solar PV the dominant energy source, while wind energy plays a complementary role, particularly during the winter months when solar irradiance is lower. The diesel generator serves primarily as a backup during extended periods of low renewable energy generation, ensuring system reliability even under adverse weather conditions [22,23].

Beyond the technical and economic dimensions, the study also examines the social and environmental impacts of transitioning to a hybrid renewable energy system [24]. Reducing diesel consumption not only cuts operating costs but also diminishes the environmental footprint of power generation in the village [25,26]. This aligns with Saudi Arabia's broader commitment to reducing carbon emissions and promoting sustainable development as part of its environmental and economic policies. The findings of this case study contribute to the growing body of

literature on the feasibility and optimization of HRES in remote and offgrid locations. The successful implementation of such systems in Saudi Arabia can serve as a model for other regions with similar climatic conditions and energy challenges. Moreover, the study underscores the potential for HRES to play a pivotal role in achieving national and global energy targets, particularly in the context of the ongoing transition to a low-carbon economy [27].

A comprehensive feasibility study was conducted on various hybrid renewable energy scenarios using advanced optimization techniques such as genetic algorithms (GA) and particle swarm optimization and other metaheuristic algorithms [28,29]. As example, optimization techniques incorporated different distributed generation strategies, revealing that an off-grid system was the most cost-effective solution among six configurations designed for Barwani, India [30,31]. Other studies have addressed the challenges associated with hybrid system design, reviewing various software tools and artificial intelligence techniques used for optimization. Further research has explored the design, integration, and optimization of smart micro-grids, focusing on the constraints and objectives related to their components. Additionally, off-grid system designs tailored for remote areas in Tamil Nadu, India, have demonstrated the feasibility of these systems in isolated regions [32,33]. An optimization and sensitivity analysis using the HOMER software was performed for four integrated renewable sources in Ukai, Gujarat, and Tamil Nadu, with several systems employing diesel generators and battery banks as backup solutions to meet the load requirements of specific areas [34-36]. An optimal design and energy management study for a fully renewable isolated microgrid integrating WT, PV, and BESS for Kanur, India, demonstrated that considering excess energy and reliability constraints, the PSO-based design achieved the lowest LCOE of 0.1229  $\$  kWh in Case-I (LOPSPmax = 5 %, PEEmax = 20 %) and 0.1020 \$/kWh in Case-II (LOPSPmax = 10 %, PEEmax = 20 %), while maintaining high supply reliability and significantly reducing greenhouse gas emissions [37].

Moreover, a comprehensive literature review necessitates the inclusion of several pertinent studies exploring various facets of renewable and hybrid energy systems. For instance, recent research has examined the adoption and awareness of renewable energy practices in specific regions like Palestine [38]. The design and optimization of hybrid systems, particularly for isolated or rural applications, have been extensively investigated, incorporating technologies such as pumped hydropower storage [39,40], diesel generators [41,42], and batteries [42]. Studies have analyzed the performance of hybrid systems for residential use [43] and explored innovative configurations like topography-based systems [44] and integrated parabolic dish solar concentrators with bioenergy [45]. Furthermore, the economic, environmental, and technical feasibility of hybrid systems, including their role in addressing power shortages [46] and their application in specific contexts like COVID-19 quarantine centers [41] or industrial electrification in Ghana [47], has been a key focus. The challenges and pathways for renewable energy transitions, considering both regional contexts like Ghana [48] and the integration of diverse sources including nuclear power [47], are also crucial areas of investigation that enrich the understanding of the current energy landscape.

Other recent studies have intensified efforts to design hybrid renewable energy systems (HRES) that balance economic feasibility, environmental sustainability, and system reliability, especially in academic, healthcare, and remote community settings. One key application has been optimizing energy systems at university campuses. For example, a techno-economic and environmental analysis conducted at a university campus demonstrated the feasibility of a grid-connected PV/Wind/DG hybrid configuration without energy storage. This system achieved a cost of energy of 0.0172/kWh and 0.0172/kWh and

integration of multi-energy sources—such as solar, wind, biogas, and hydrogen-into multi-microgrid configurations has shown improved system reliability and resource utilization. A distributed dynamic economic dispatch model considering microgrid selfishness was proposed, enabling efficient coordination across multiple decentralized microgrids [50]. For rural and off-grid communities, renewable-based microgrids remain essential. A study in rural Bangladesh designed a PV/WT/BESS system with a COE of \$0.0688/kWh and zero emissions, highlighting scalability for future demand [51]. Similarly, networked microgrids with layered control and predictive deep learning-based energy management strategies have demonstrated robust grid support capabilities across variable conditions [52]. Healthcare facilities also benefit significantly from HRES adoption. An optimized PV/WT/BESS/DG system showed a 76.8 % reduction in total NPC and significant emission cuts, although low wind speeds in the deployment region limited the economic viability of wind integration [53]. Campus microgrids, like those analyzed for the VIT Chennai campus, combine solar, wind, diesel, and battery systems to meet growing energy demand. Such systems drastically reduce carbon emissions and offer flexible grid-tied and standalone operation modes [54]. In rural African settings, hybrid PV/ Wind systems integrated with TES and PHES also demonstrated high reliability and cost-efficiency, especially when optimized using advanced metaheuristic algorithms and reliability indices like loss of power supply probability (LPSP) [55]. Collectively, these studies demonstrate that hybrid renewable energy systems, when tailored to site-specific conditions and application demands, provide viable and scalable solutions for achieving sustainable energy across both gridconnected and off-grid settings.

The optimization of Hybrid Energy Systems (HES) using the Cycle Control (CC) strategy and other control strategies within the HOMER software has been extensively explored in various research studies across different geographical locations, including India, Taiwan, Australia, Indonesia, and more. Kumar et al. (2020)[56] conducted a simulation in Delhi, India, focusing on a solar-diesel-battery HES, demonstrating that the CC strategy reliably meets load demands while minimizing the Net Present Cost (NPC). Hong and Magararu (2021) [57] applied the CC strategy in Taiwan to optimize a hybrid system with PV, wind, hydro, and non-renewable sources, finding that increased renewable energy reduces carbon emissions but raises system costs. Das and Hasan (2021) [58] compared the Load Following (LF) and CC strategies in South Wales, Australia, concluding that while CC offers superior environmental and economic benefits, LF provides a higher renewable fraction. Ramesh and Saini (2020) [59] in Karnataka, India, found that the co-dispatch strategy was most cost-effective for lithiumion battery HES. Azahra et al. (2020) [60] evaluated an off-grid solardiesel-battery HES in Indonesia, finding that CC provides better economic performance, though LF allows for more renewable energy. Sharma and Mishra (2019) [61] proposed a solar-biomass-battery HES for a university campus in India, showing it was both technically feasible and cost-effective. In Turkey, Polat and Sekerci (2021) [62] found that the CC strategy resulted in lower NPC and cost of energy (COE) for villas in Izmir. Malanda et al. (2021) [63] assessed the feasibility of an off-grid HES in Malawi, finding optimal performance with solar/wind/battery systems for remote electrification. Kumar et al. (2018) [64] optimized HES designs for off-grid and grid-connected systems at a university campus in India, highlighting the dominance of solar panels. Fofang and Tanyi (2020) [65] in Cameroon concluded that the CC strategy had a lower NPC for a solar-hydro HES. Rezk et al. (2020) [66] found that the LF strategy offered better economic performance for a standalone solardiesel-battery system in Minya City, Egypt. Mubaarak et al. (2020) [67] proposed an off-grid solar-wind-diesel-battery HES for Taiz Province, Yemen, which was economically viable under the CC strategy. Das et al. (2020) [68] in Bangladesh found that the LF strategy resulted in lower COE and NPC for a grid-connected solar-battery HES. Javid et al. (2020) [69] in Pakistan found both LF and CC strategies viable for an industrial facility in Faisalabad. Soon et al. (2019) [70] in Malaysia showed that

optimal HES configurations were achieved using the LF strategy. Popoola et al. (2021) [71] concluded that a solar-wind-diesel-battery HES was superior to a diesel generator system for powering the University of Ilorin Library in Nigeria, in both economic and environmental aspects. A recent study presented a techno-economic assessment of hybrid renewable energy systems integrating battery and hydrogen storage, showing that a WT/PV/FC/Electrolyzer/HSS/BES configuration designed in HOMER achieved the lowest net present cost and cost of energy with improved reliability in isolated microgrids [72]. Moreover, A comprehensive study on hybrid renewable energy systems for isolated rural microgrids using HOMER demonstrated that integrating locally available renewable resources with storage and backup generation provides a technically viable and economically optimal solution, achieving lower cost of energy, reduced greenhouse gas emissions, and improved supply reliability, thereby supporting rural electrification and national climate targets [73]. A techno-economic and sensitivity analysis of a standalone hybrid energy system for Kanur village in India, designed in HOMER with PV, WT, DG, and BES, showed that the optimal PV/WT/DG/BES configuration achieved the lowest net present cost of 569,275 \$ and cost of energy of 0.157 \$/kWh with zero capacity shortage, while sensitivity results indicated that variations in discount and inflation rates strongly affect economic feasibility, emphasizing the need for careful parameter selection in microgrid planning [74]. Table 1 lists numbers of HESS optimization studies.

#### 1.2. Research gap

The literature review highlights the critical role that integrated renewable energy sources play in providing electricity to remote locations. Recently, Saudi Arabia has emphasized the importance of off-grid electrification using renewable sources for remote and poorly electrified rural areas. However, reliance on single renewable energy generators often leads to a mismatch between load and demand, resulting in poor economic viability and low renewable energy penetration. To address these challenges and enhance economic efficiency and renewable energy integration, this article aims to design an electrification system for a remote area in Najran, which boasts rich solar and wind resources. While some studies have focused on the techno-economic assessment of PV/wind/battery hybrid systems for domestic loads in other regions of Saudi Arabia, comprehensive studies on these systems for Najran are limited. Therefore, the primary objective of this study is to explore offgrid HRES configurations across different locations in Najran, seeking the most effective combination of available renewable sources to provide reliable and sustainable electricity.

The focus of this paper is to build on existing studies by conducting a comprehensive feasibility analysis of hybrid renewable energy systems in a specific case study located in Saudi Arabia. Given the country's vast geographic expanse and varying climatic conditions, implementing OFFGPS presents unique challenges and opportunities. This study aims to explore the optimal configuration of an OFFGPS that integrates solar, wind, and diesel generation to meet the energy needs of a remote community in Saudi Arabia. The analysis includes a detailed examination of system costs, maintenance requirements, subsidies, and benefits, as well as the design, simulation, and optimization of the proposed system using the HOMER software tool. The findings will contribute to the growing body of knowledge on the deployment of hybrid renewable energy systems in diverse environments and provide valuable insights for policymakers, engineers, and stakeholders involved in the electrification of remote areas.

#### 1.3. Contribution of research

The key contributions of this research are as follows:

 A novel off-grid PV/Wind/Diesel/Battery hybrid energy system is developed and optimized for remote regions in Sharurah, Saudi

**Table 1**Overview of HESS optimization studies.

Year	Ref.	Location	Configuration	Strategy	Grid Type	Evaluation Metrics
2018	Kumar et al. [64]	University Campus, India	PV-Biogas-Diesel- Battery	LF, CC	Off-Grid, On-Grid	The study evaluated the system's performance based on NPC and COE.
2019	Soon et al. [70]	Rural Area, Malaysia	PV-Hydro-Diesel- Battery	LF, CC	Off-Grid	The evaluation considered NPC, COE, electricity production, and fuel consumption.
2019	Sharma and Mishra [61]	University Campus, India	PV-Biomass-Battery	CC	On-Grid	The study assessed the system using NPC and COE as key metrics.
2020	Kumar et al.	Delhi, India	PV-Wind-Diesel- Battery	CC	Off-Grid	The evaluation focused solely on NPC.
2020	Ramesh and Saini [59]	Karnataka, India	PV-Wind-Hydro- Diesel-Battery	LF, CC	Off-Grid	The system's effectiveness was measured through NPC, COE, CO2 emissions excess power, and capacity shortage.
2020	Azahra et al. [60]	Small Island, Indonesia	PV-Diesel-Battery	LF, CC	Off-Grid	The analysis considered NPC, CO2 emissions, renewable energy fraction, fue consumption, battery performance, and excess power.
2021	Malanda et al. [63]	Villages, Malawi	PV-Wind-Diesel- Battery	CC	Off-Grid	The study evaluated the system's performance based on NPC and COE.
2020	Fofang and Tanyi [65]	Rural Area, Cameroon	PV-Hydro-Battery	LF, CC	Off-Grid	The evaluation metrics included NPC and COE.
2020	Rezk et al. [66]	Minya City, Egypt	PV-Diesel-Battery	LF, CC	Off-Grid	The performance was assessed based on NPC, COE, emissions, electricity production, fuel consumption, and battery performance.
2020	Mubaarak et al. [67]	Taiz Province, Yemen	PV-Wind-Diesel- Battery	CC	Off-Grid	The system was evaluated using NPC, COE, emissions, electricity production renewable energy fraction, fuel consumption, performance, and excess power.
2020	Javid et al. [69]	Faisalabad, Pakistan	PV-Diesel-Biodiesel- Battery	LF, CC	Off-Grid	The study considered NPC, COE, unmet load, capacity shortage, and emissions as key evaluation metrics.
2020	Das et al. [68]	Rajshahi, Bangladesh	PV-Battery	LF, CC	On-Grid	The system's performance was measured based on NPC, COE, grid purchases excess power, and capacity shortage.
2021	Das and Hasan [58]	South Wales, Australia	PV-Wind-MGT- Battery	LF, CC	Off-Grid	The study evaluated NPC, CO2 emissions, renewable energy fraction, fuel consumption, battery performance, and excess power.
2021	Polat and Sekerci [62]	Villas, Izmir, Turkey	PV-Wind-Diesel- Battery	LF, CC	Off-Grid	The system was assessed based on NPC, emissions, electricity production, fuel consumption, battery performance, and excess power.
2021	Popoola et al. [71]	University of Ilorin, Nigeria	PV-Wind-Diesel- Battery	CC	Off-Grid	The evaluation focused on NPC, COE, and emissions.
2021	Hong and Magararu [57]	Various Areas, Taiwan	PV-Wind-Hydro- Nonrenewable	CC	On-Grid	The performance was evaluated based on NPC, COE, renewable energy fraction, operating cost, and CO2 emissions.
2022	Ali Saleh et al. [75]	Al Anbar, Iraq	PV-Diesel-Battery	CC, Author Str.	Off-Grid	The system's effectiveness was assessed using NPC, COE, emissions, electricity production, renewable energy fraction, fuel consumption, capacity shortage, unmet load, and battery performance.

Arabia, targeting minimum cost and high renewable energy penetration.

- The study evaluates the performance of multiple configurations using three dispatch strategies—Cycle Charging (CC), Load Following (LF), and a proposed MATLAB-linked (ML) strategy—based on Net Present Cost (NPC) and Cost of Energy (COE).
- A detailed sensitivity analysis is performed to assess the impact of diesel fuel price variations on system cost and performance.
- The optimized system demonstrates high renewable fraction, reduced emissions, and strong environmental benefits, offering a sustainable solution for off-grid applications.

#### 1.4. Organization

The remainder of this paper is structured as follows: Section 2 describes the case study. Section 3 outlines the system components. Section 4 details the modeling of the proposed microgrid configuration. Section 5 presents the control strategies. Section 6 discusses the results. Finally, Section 7 concludes the paper.

# 2. Case study

#### 2.1. Location

This research investigates two regions with distinct renewable energy potentials. The area studied in the Najran city is characterized by its low electricity distribution coverage. Sharurah is a town situated in the Najran Province of southern Saudi Arabia, roughly 200 miles east of the

city of Najran. The location of case study has been shown in Fig. 1. Positioned within the Empty Quarter desert near the Yemeni border, Sharurah serves primarily as a border town. According to the 2022 Census, the population of Sharurah is approximately 170,000. The town's geographic coordinates are  $17^{\circ}29^{\prime}N$  latitude and  $47^{\circ}07^{\prime}E$  longitude.

#### 2.2. Load profile

Accurate estimation of energy demand is vital for effective energy planning. Sharurah has a peak electrical load of 3899.5 W, with peak energy consumption occurring between 12 PM and 10:00 PM. Load profiles for this district are detailed in terms of annual and hourly demand, illustrating energy consumption patterns over a 24-hour period have been shown in Fig. 2.

#### 2.3. Solar irradiance

(Fig. 3.A) presents the global horizontal irradiation map of saudi arabia, highlighting that the sharurah region receives high levels of solar radiation [76]. Sharurah's solar potential was assessed using data collected over a year from NASA, as shown in Fig. 3.b. The solar irradiance is with an annual average of 6.38 kWh/m2 per day. This indicates a strong potential for solar energy generation despite the region's limited wind resources. May experiences the highest solar radiation at 7.21 kWh/m2 per day, while December records the lowest at 5.21 kWh/m2 per day. This suggests that even during months with lower solar radiation, there is sufficient sunlight for effective solar power



Fig. 1. The location of the case study.

generation.

#### 2.4. Wind resources

Saudia Arabia has access to moderate wind resources. Based on 39 years of national wind data, wind speeds in parts of southern Saudi Arabia, including Sharurah, range between 5–6.4 m/s at 50 m height as shown in Fig. 4.a [77]. The recorded data values are suitable for hybrid energy systems. The wind data was spatially mapped using advanced interpolation methods, ensuring accuracy and regional relevance. In Sharurah, wind resource from NASA and the National Renewable Energy Laboratory (NERL) assessment demonstrates that the wind speeds with an average annual wind speed of 4.24 m/s. This suggests that the district has significant potential for wind energy utilization, as shown in Fig. 4.

# 3. System description and components

This study utilized HOMER software to analyze and quantify the costs associated with various controlling methods of the hybrid power system, encompassing off-grid configuration. For a comprehensive evaluation, HOMER requires precise input data to assess optimization results across different system combinations. Our focus included evaluating the performance of photovoltaic (PV) systems, wind turbines (WT), and diesel generators (DG). Battery energy storage systems (BESS) were selected due to their high efficiency (typically 85–95 %), rapid dynamic response, and low operational and maintenance requirements. Unlike pumped-hydro or thermal storage, BESS can be easily scaled and deployed in remote areas where space and water availability are limited. Additionally, batteries offer seamless integration with PV and wind systems, enabling short-term load balancing and frequency regulation. These attributes make BESS a practical and cost-effective choice for hybrid renewable energy systems, especially in isolated microgrids or rural environments.

The proposed hybrid power system integrates several key components, as depicted in Fig. 5:

- AC Bus Side: Wind turbines and the diesel generator are connected to the AC bus, supplying power to the AC network.
- DC Link Side: Solar PV systems and energy storage devices are linked to the DC side, where they provide renewable energy and store excess power.

In this configuration, solar PV and wind systems serve as the primary renewable energy sources, while the diesel generator acts as a backup to meet power demands during periods of insufficient solar or wind resources. The energy storage system ensures a consistent power supply during high load periods or times of reduced resource availability, enhancing the system's overall reliability. A power converter manages

and regulates the electricity flow to ensure it is suitable for consumer use. Detailed cost information for each component, including initial investment, replacement, and operational and maintenance costs, is provided in Table 2 [78–80]. The selected PV modules and wind turbines have been chosen based on their proven performance in arid and semi-arid climates. Specifically, monocrystalline PV modules have been preferred due to their higher efficiency under high irradiance and elevated temperatures, which align with findings reported in [81]. For wind energy, medium-scale horizontal-axis turbines have been selected based on their low carbon footprint and favorable energy life cycle assessment in similar regions [82]. The choice of DC-AC converters has been guided by efficiency, modularity, and cost-effectiveness, ensuring system compatibility and optimal operation. Furthermore, solar radiation modeling has been aligned with the transposition models validated in [52] to enhance the accuracy of input data for the PV system (Table 3)

# 4. Modeling of the suggested MG configuration

#### 4.1. PV Plant

Solar energy is a virtually limitless source of power. For this study, CS6U-330P polycrystalline solar cells were selected, each with a nominal maximum power of 0.330 kW. A derating factor and ground reflectance values of 88 % and 20 %, respectively, were applied. In HOMER, users need to include a report detailing the solar resource, which reflects how much solar energy reaches the earth's surface over a year. The clearness index represents the ratio of local irradiation to calculated extraterrestrial irradiation at the location. The photovoltaic output performance is calculated as the following [83]:

$$P_{pv} = Y_{pv} \times F_{spv} \times \frac{G_t}{G_{stc}} \times \left[ 1 + \alpha_p \left( T_c - T_{c,stc} \right) \right]$$
 (1)

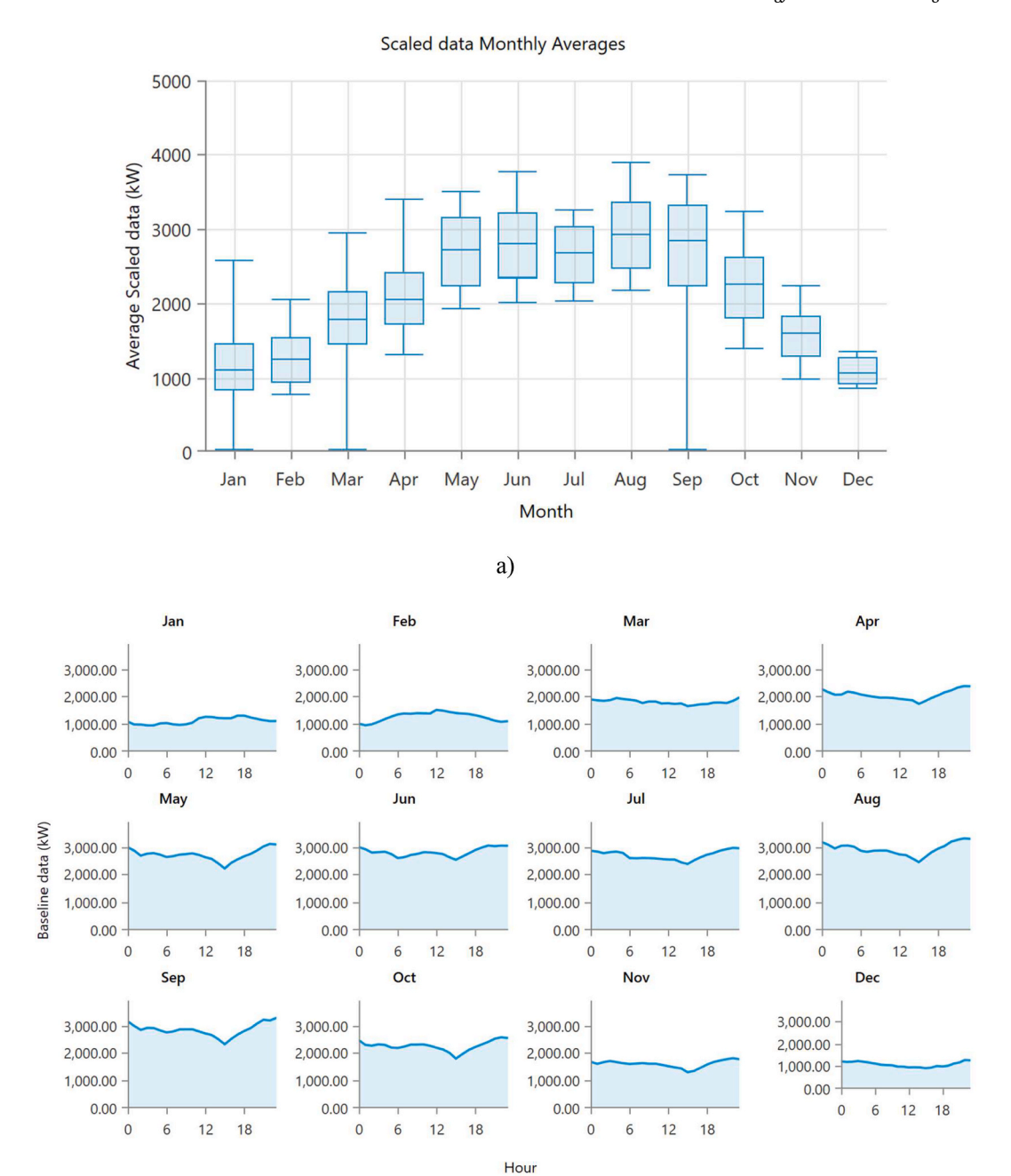
where  $Y_{pv}$  is the solar power capacity in kW,  $F_{spv}$  is the solar derating factor,  $G_t$  is the incident solar radiation on the PV array (kW/m²),  $G_{stc}$  is the standard test condition solar radiation (1 kW/m²),  $\alpha_p$  is the temperature coefficient based on power,  $T_{c,stc}$  is the cell temperature under standard test conditions (25 °C) and  $T_c$  is the cell temperature. Moreover, the cell temperature  $T_c$  can be represented as follows [84]:

$$T_{\text{cell}} = T_{\infty} + 7 \times 10^{-2} \frac{G_t}{1000} \tag{2}$$

where  $T_{\infty}$  represents the air temperature in (°C).

# 4.2. Wind turbine power plant

Wind energy is advantageous due to its potential as a clean energy source with minimal pollution. For this study, a generic 1 kW wind turbine model with a 17-meter hub height was selected and simulated



b)

Fig. 2. Load profiles for the district, illustrating a) annual and b) hourly energy consumption patterns over a 24-hour period.

using HOMER. The software requires wind resource data, including the range of wind speeds expected over a year. HOMER calculates the wind turbine's power output using a four-phase process: determining the average hourly wind speed, adjusting for hub height using logarithmic or power laws, applying the power curve of the turbine, and adjusting for actual air density. The wind speed at hub height is calculated as follows [9,85]:

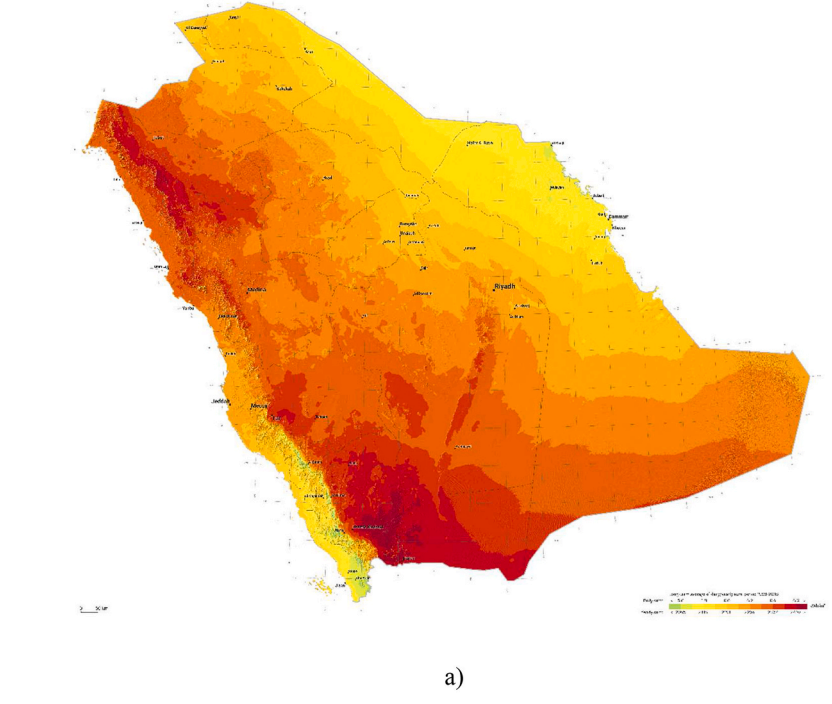
$$W_{s,hub} = W_{s,anem} \times \left(\frac{Z_{hub}}{Z_{anem}}\right)^{a} \tag{3}$$

where  $W_{s,hub}$  is the wind speed at hub height,  $W_{s,anem}$  is the wind speed at anemometer height,  $Z_{hub}$  is the hub height,  $Z_{anem}$  is the anemometer height, and  $\alpha$  is the power law exponent i.e. the wind shear coefficient. The maximum power output of the wind turbine is determined by Eq.

$$P_{wtg} = \frac{\rho}{\rho_0} \times P_{wtg,stp} \tag{4}$$

where  $P_{wtg}$  is the turbine's maximum output power,  $\rho$  is the actual air density,  $\rho_0$  is the standard air density, and  $P_{wtg,stp}$  is the power output at standard temperature and pressure.

The energy production be a certain wind turbine is estimated as [86,87]:



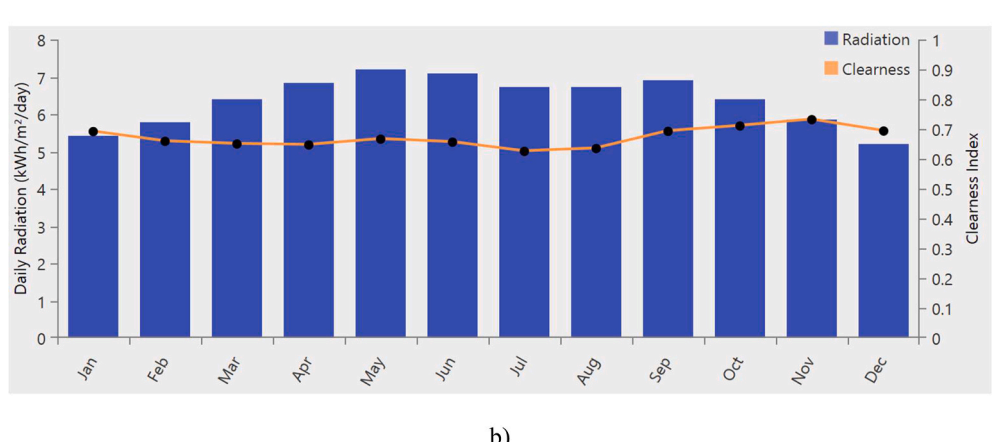


Fig. 3. A) the global horizontal irradiation map of saudi arabia and b) solar potential was assessed using data collected over a year.

$$E_{W} = \begin{cases} P_{wtg.stp} \\ P_{wtg.stp} \left( \frac{V_{Z,t} - V_{cut-in}}{V_{rat} - V_{cut-in}} \right) & W_{rat} \leq W_{s,hub} \leq W_{cut-off} \\ W_{cut-in} < W_{s,hub} \leq W_{rat} \\ W_{s,hub} \leq W_{cut-in}ORW_{s,hub} > W_{cut-off} \end{cases}$$
(5)

where  $P_{wtg,stp}$  represents the rated power of the wind turbine at rated wind speed  $W_{rat}$ ,  $W_{cut-in}$  and  $W_{cut-off}$  denote the cut-in and cut-off wind speeds, respectively.

#### 4.3. Diesel generator system

Diesel generators are commonly used for remote electrification due to their cost-effectiveness, ease of installation, and operational simplicity. They are reliable sources of backup power with a quick start-up time compared to other technologies. For this study, a 13-kW diesel generator with a minimum load ratio of 25 % was modeled using HOMER. Fuel consumption is considered as follows [88]:

$$F = F_0 \times Y_{gen} + F_1 \times P_{gen} \tag{6}$$

where  $F_0$  is the intercept of the fuel curve,  $F_1$  is the slope,  $Y_{gen}$  is the rated

power, and  $P_{gen}$  is the power output. HOMER calculates both fixed and marginal energy costs of the generator, where the fixed costs are the operating expenses per hour without generating power, and the marginal cost is the additional cost per kilowatt-hour of extra output. The fixed energy cost is designed as follows:

$$G_{ec} = C_{om,g} + \frac{C_{rep,g}}{R_g} + F_0 \times Y_g \times C_{eff,fc}$$
 (7)

where  $C_{om,g}$  is the service and repair cost per hour,  $C_{rep,g}$ , is the replacement cost,  $R_g$  is the generator lifespan,  $Y_g$  is the generator power capacity, and  $C_{eff,fc}$  is the effective fuel cost. The marginal energy cost is calculated as follows:

$$C_{gen,mar} = F_1 \times C_{eff,fc} \tag{8}$$

where  $F_1$  is the slope of the fuel curve and  $C_{eff,fc}$  is the effective fuel cost.

#### 4.4. Battery storage units

Energy storage technologies, including batteries, collect and store electrical energy for later use, thereby enhancing system efficiency and

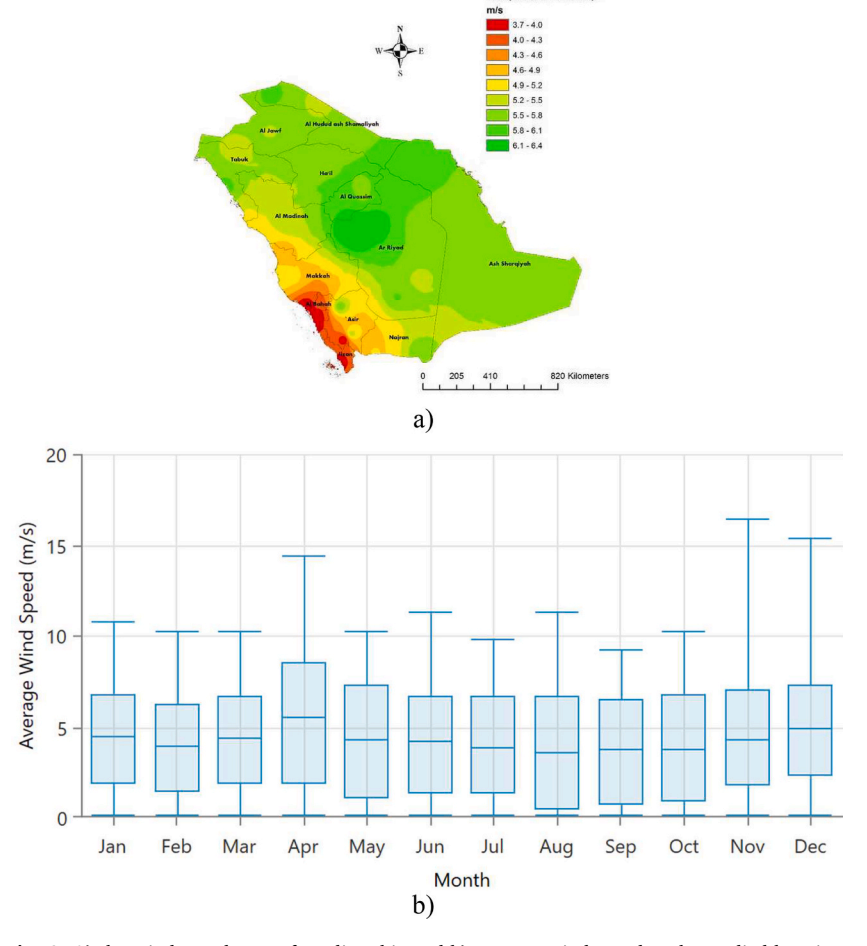
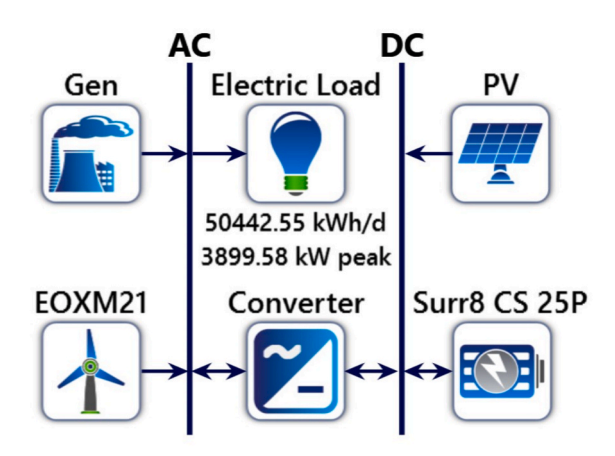


Fig. 4. A) the wind speed map of saudi arabia and b) average wind speed at the studied location.



 $\textbf{Fig. 5.} \ \ \textbf{The studied configuration of the hybrid energy system in HOMER.}$ 

stability by matching supply with demand. In this study, a kinetic battery model with a 5-year lifespan was used. The battery's minimum state of charge is 20 %, and the initial charge is 100 %. The state of charge (SOC) is calculated using the following equation [89]:

$$SOC = \frac{C_b}{C_m} \tag{9}$$

where  $C_b$  is the battery capacity and  $C_m$  is its maximum capacity. The depth of charge (DOC) is calculated using Equation (10):

**Table 2** Designed data of the hybrid energy system [78].

Component details	PV system	Wind system	Generator	Battery	Converter
Capital costs (S)	469.03/ kW	997/kW	230/kW	216.78/ Battery	65/kW
Replacement costs (\$)	469.03/1 < W	997/kW	230/kW	160.47/ Battery	65/kW
O and M costs (S)	150/Year	150/ Year	0.5/hr	5/Year	10 Year
Component life	25 Years	20 Years	15,000 h	5 Years	15 Years

$$DOC = SOC - 1 \tag{10}$$

where *DOC* is the depth of charge and *SOC* is the state of charge. To protect against deep discharging and overcharging, the battery capacity is constrained by Equation (11):

$$C_{min} \le C_t \le C_{max} \tag{11}$$

where  $C_t$  is the current battery charge, and  $C_{max}$  and  $C_{min}$  are the maximum and minimum capacities, respectively. Moreover, the energy level (SoC(t)) over the time step can be represented as the following [86]:

$$SoC(t) = SoC(t-1).(1-\sigma) + \left(P_{in}(t) - \frac{P_{out}(t)}{\eta_{inv}}\right) \times \eta_b \tag{12}$$

where  $\sigma$  denotes the battery energy self-consumption 1%/day. The

**Table 3**The dispatch strategies and component sizes for the optimized configurations.

Component	Unit	Dispatch Strat	Dispatch Strategy						
		Base Case	HOMER Cycle Charging	HOMER Load Following	HOMER Pro MATLAB Link Without DG With DG				
Generator	Autosize Genset, kW	4,300	4,300	4,300	None	4,300			
PV	kW	None	5,450	7,562	14,091	5,533			
Wind Turbine	Eocycle EOX M-21 [100 kW]	None	57	32	26	71			
Storage	Surrette 8 CS 25P, strings	None	5,476	5,361	15	47			
Converter	kW	None	3,058	3,573	5,823	3,106			

symbols of  $P_{in}(t)$  represents energy charging while the  $P_{out}(t)$  represents energy discharging. Moreover,  $\eta_{inv}$  represents the inverter efficiency while the  $\eta_b$  represents the battery efficiency.

#### 4.5. Inverter modelling

The inverter rated power may be represented as follows to meet the load conditions [90]:

$$P_{inv}(t) = \frac{P_l(t)}{\eta_{inv}} \tag{13}$$

where  $P_{inv}$  is the designed rated power and  $P_l$  is the load power. Moreover, the rated power of the selected inverter in the HOMER Pro is optimized as one of the optimized variables.

#### 4.6. Mathematical economic modeling of the MG

HOMER calculates the total NPC by incorporating capital, replacement, maintenance, fuel costs, and other expenses. This comprehensive financial analysis reflects both the gross current net expense and the cost of electricity. The net life cycle cost can be calculated as:

$$CNPC = C_{ann,tot} \times CRF(i, R_{proj})$$
 (14)

where  $C_{ann,tot}$  is the total annualized expense, i is the real discount rate,  $R_{proj}$  is the project lifespan, and CRF is the capital recovery factor. The capital recovery factor is given as the following equation:

$$CRF(i,N) = \frac{i}{(1+i)^N} \left( \frac{(1+i)^N - 1}{i} \right)$$
 (15)

where N is the number of years and i is the real discount rate. The real discount rate is calculated from the nominal discount rate and inflation rate using Equation (16):

$$i = i' - \frac{f}{1+f} \tag{16}$$

where i' is the nominal discount rate and f is the inflation rate.

#### a) Cost of energy expenses

The cost of energy, or the average price per kilowatt-hour, is determined by Equation (17):

$$COE = \frac{C_{annual,total}}{E_{primary} + E_{deferable} + E_{grid,sales}}$$
 (17)

where  $C_{annual,total}$  is the total annualized cost,  $E_{primary}$  and  $E_{deferable}$  are the amounts of primary and deferrable load served, and  $E_{grid,sales}$  is the annual electricity supplied to the grid.

#### b) Environmental Criteria.

Environmental impact, particularly carbon emissions, is a critical

factor in hybrid system configurations. The total CO2 emissions are calculated using Equation (18):

$$TCO_2 = 3.667 \times V_f \times X_c \times F_{hv} \times F_{cef}$$
 (18)

where  $TCO_2$  is the total CO2 emissions,  $V_f$  is the fuel consumption in liters,  $F_{hv}$  is the heating value of fuel (MJ/L),  $F_{cef}$  is the carbon emission factor (toncarbon/TJ), and  $X_c$  is the fraction of carbon oxidized.

The environmental cost associated with  $CO_2$  emissions, denoted as  $C_{CO2}$ , to provide a direct measure of the economic impact of  $CO_2$  emissions associated with energy production, may be estimated as follows [91]:

$$C_{CO2} = EF_{CO2} \times E_t \times \Phi_{CO2} \tag{19}$$

where  $EF_{CO2}$  is the  $CO_2$  emission factor of the power generation system, expressed in kg  $CO_2$  per kWh.  $E_t$  is the total electrical energy generated in kWh.  $\Phi_{CO2}$  is the social cost of carbon, representing the economic cost of  $CO_2$  emissions in (\$/ton)  $CO_2$ . A representative value for  $\Phi_{CO2}$  is (\$70/ton)  $CO_2$  [92].

#### c) Renewable fraction calculation

The renewable fraction represents the proportion of electricity supplied from renewable sources. It is calculated using Equation (20):

$$F_{renewable} = 1 - \frac{E_{nonren} + H_{nonren}}{E_{served} + H_{served}}$$
 (20)

where  $F_{renewable}$  is the renewable fraction,  $E_{nonren}$  and  $H_{nonren}$  are the nonrenewable electrical and thermal energy produced, and  $E_{served}$  and  $H_{served}$  are the total electrical and thermal loads served.

#### 5. Control strategies

Over recent decades, various tools have been utilized to analyze the technical, economic, environmental, and socio-political aspects of renewable energy technologies. Among these, the Hybrid Optimization of Multiple Energy Resources (HOMER) tool, developed by the National Renewable Energy Laboratory in the United States, has been widely used [18]. Its popularity stems from its accuracy, simplicity, and speed in sizing and optimizing hybrid renewable energy systems (HRES). HOMER Pro is valued for its dual capability to perform financial and technical analyses and its applicability in both on-grid and off-grid microgrid modeling, despite its steep learning curve [93,94].

HOMER Pro operates by processing inputs such as resource data, load profiles, economic information, microgrid constraints, and control strategies. It then optimizes the hybrid system and provides outputs including net present cost, component sizes, cost of energy, excess electricity, unmet load, and return on investment [18]. The software models the system using two primary approaches: component modeling to project electricity production and economic modeling to assess feasibility. A critical aspect of optimization is balancing electricity production with associated costs over the microgrid's lifecycle. To identify the best configuration, renewable energy ratios, and optimal system sizes, HOMER Pro compares system output variables against

economic parameters. The effectiveness of the optimal system configuration is significantly influenced by the power management strategy, with most studies using a load-following approach for sizing and performance analysis.

The Controller component in HOMER Pro allows users to define how the system operates during simulations by selecting different control algorithms or dispatch strategies. HOMER Pro supports various strategies, including CC, LF, MATLAB Link (ML), Generator Order (GO), Combined Dispatch (CD), and Predictive Dispatch (PS) [18,94]. Each strategy is optimized during simulation, enabling users to compare their performance. For example, Cycle Charging runs generators at full capacity to charge batteries, while Load Following only produces enough power to meet demand, making it suitable for systems with high renewable energy.

In this paper, two well-established dispatch strategies, CC and LF, have been applied to assess the system's performance. Additionally, a novel strategy has been introduced using MATLAB Link (ML), showcasing an innovative approach to optimizing the hybrid energy system. The framework of MG optimization in HOMER has been shown in Fig. 6.

#### 5.1. Cycle charging strategy

Fig. 7 illustrates the CC dispatch strategy for the PV//wind/diesel/battery system. While this strategy operates similarly to the LF dispatch strategy, it diverges in the operational specifics. The generator's maximum rated capacity is utilized when it is active to meet the net load and charge the battery with any excess energy. This figure depicts the operation of the cycle charging strategy, coordinating between photovoltaic (PV) panels, wind turbines, a diesel generator, and battery storage to meet energy demand [95]. Fig. 7 highlights how renewable energy sources are prioritized, while the diesel generator provides backup, with the battery storage balancing excess generation and supply shortages throughout different periods of operation. The following equations are used to describe the cost implications of each decision.

#### a. Battery discharge cost

The cost of discharging the batteries is given by:

$$C_{\text{discharge}} = C_{\text{batt, wear}} + C_{\text{batt, energy}} \tag{16}$$

where  $(C_{\mathrm{batt,\; energy}})$  represents the battery energy cost, calculated at time step (n) as:

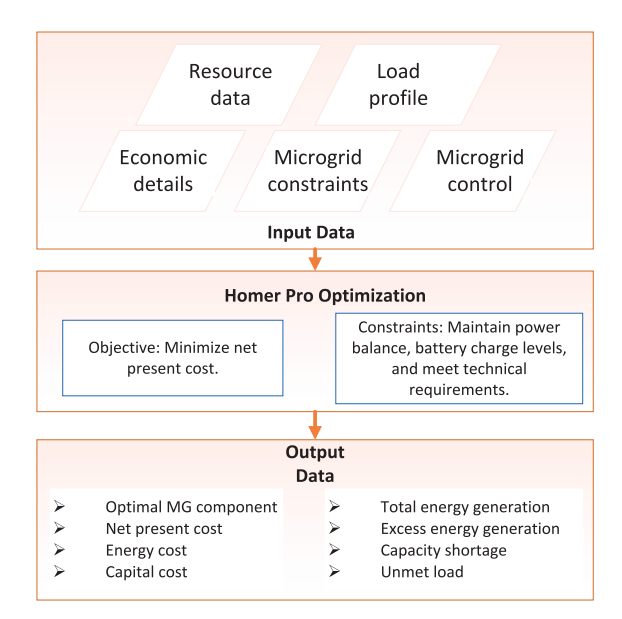


Fig. 6. Framework of MG optimization in HOMER.

$$C_{\text{batt, energy},n} = \frac{\sum_{i=1}^{n-1} C_{\text{cc},i}}{\sum_{i=1}^{n-1} E_{\text{cc},i}}$$
(17)

where,  $(C_{cc,i})$  denotes the cycle charging cost at time step (i), and  $(E_{cc,i})$  is the amount of energy charged into the batteries at time step (i) (kWh).

#### b. Generator operation cost

The cost of operating the generator at maximum capacity to cover the net load and charge the battery is given by:

$$C_{\text{gen, ch}} = C_{\text{gen}} + C_{\text{cc}} - C_{\text{batt, energy}}$$
 (18)

where  $(C_{cc})$  is the cycle charging cost for the current time step, computed as:

$$C_{\rm cc} = C_{\rm gen, \, marg} + C_{\rm batt, \, wear} \tag{19}$$

#### c. Marginal cost of the generator

The marginal cost of the generator is calculated as:

$$C_{\text{gen, marg}} = \frac{F_{\text{slope}} \times F_{\text{price}}}{\eta_{\text{rt}}}$$
 (20)

where  $(F_{slope})$  represents the slope of the fuel cost curve (L/kWh),  $(F_{price})$  is the fuel price (\$/L), and  $(\eta_{rt})$  is the round-trip efficiency.

#### d. Operational cases

The CC dispatch strategy for meeting the electrical load can be summarized into three scenarios:

- 1. PV and wind Generation Equals Demand: When PV and wind generation matches the electricity demand, the load is entirely met by PV power. In this case, the generator remains off, and the battery remains idle, resulting in surplus electricity.
- Excess PV and wind Generation: If PV and wind generation exceeds the electricity demand, the surplus energy is used to charge the battery.
- 3. Insufficient PV and wind Generation: If PV and wind generation alone cannot meet the demand, two sub-cases arise:
- Battery SOC Low: If the battery SOC is below the acceptable threshold, the generator operates near its maximum capacity to supply the remaining power (net load). The battery charges with excess generator power.
- Battery SOC High: If the battery SOC is above the acceptable threshold, two options are considered:
- The generator meets the remaining power needs and charges the battery if its output power exceeds the net load and is cost-effective compared to battery discharge.
- Alternatively, the battery discharges to meet the remaining power needs if its discharge power is sufficient and more cost-effective than running the generator. If the battery cannot meet the load alone, the generator is activated to assist.

The cost of these decisions is quantified as:

· Battery Discharging Cost

The cost of discharging the battery is calculated by:

$$C_{\text{discharge}} = C_{\text{batt, wear}} + C_{\text{batt, energy}}$$
 (21)

where  $(C_{\text{batt. wear}})$  is the wear cost, estimated as:

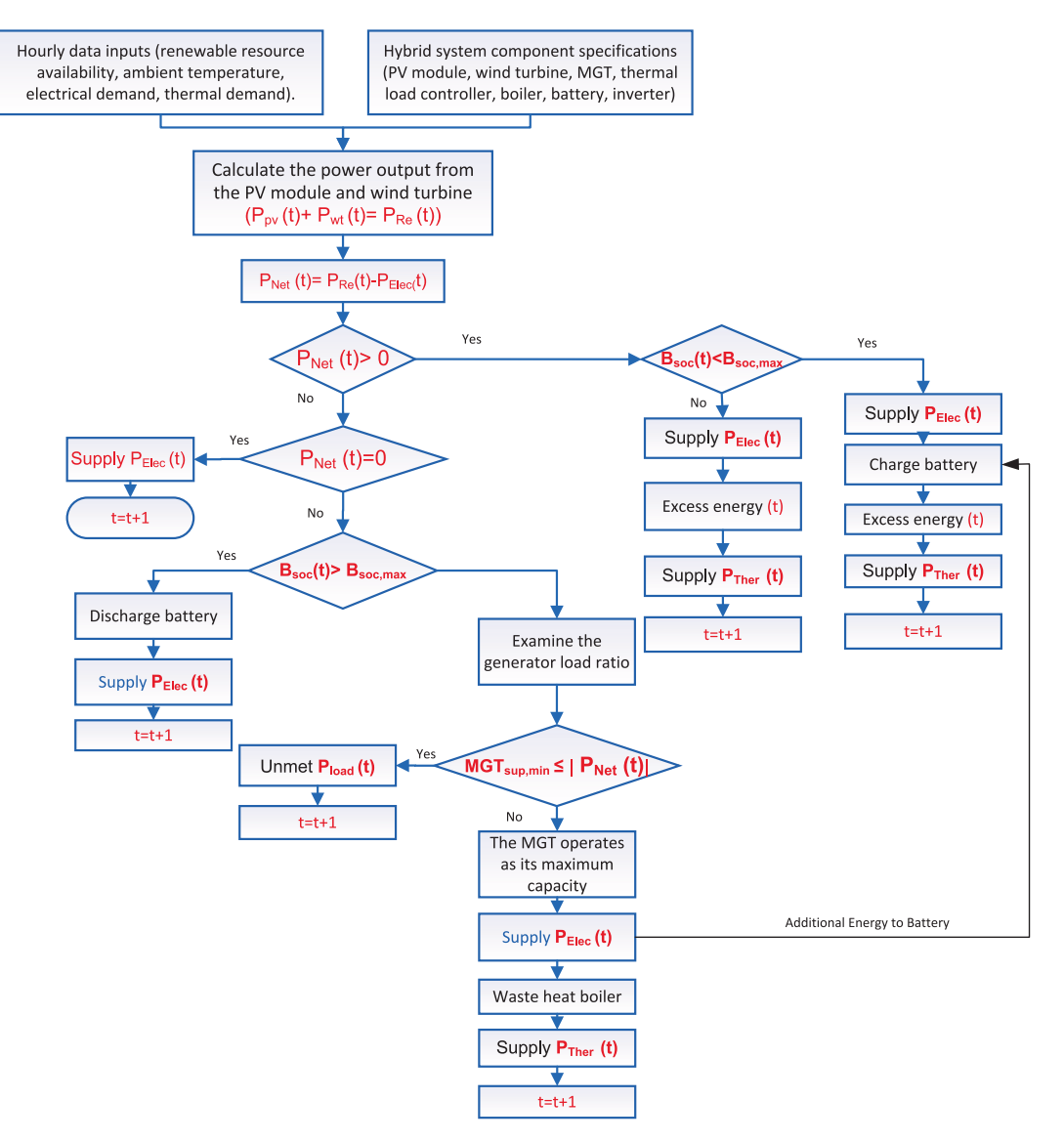


Fig. 7. The CC dispatch strategy for the PV/Wind/Diesel/Battery System.

$$C_{\text{batt, wear}} = \frac{BRC}{N \times \text{ST} \times \text{RE}}$$
 (22)

with (BRC) as the battery replacement cost, (N) as the number of batteries, ST as the single storage throughput, and RE as the storage round-trip efficiency.

• Battery Energy Cost

The battery energy cost  $(C_{\text{batt, energy}})$  at time step (m) is given by:

$$C_{\text{batt, energy},m} = \frac{\sum_{i=1}^{m-1} C_{\text{cc},i}}{\sum_{i=1}^{m-1} E_{\text{cc},i}}$$
(23)

• Generator Cost for Net Load and Battery Charging

The cost of running the generator to cover the net load and charge the battery is:

$$C_{\text{gen, ch}} = C_{\text{gen}} + C_{\text{cc}} - C_{\text{batt, energy}}$$
 (24)

where  $(C_{cc})$  is computed as:

$$C_{\rm cc} = C_{\rm gen, \, marg} + C_{\rm batt, \, wear} \tag{25}$$

e. Generator marginal cost

The marginal cost of the generator is:

$$C_{\text{gen, marg}} = \frac{F_{\text{slope}} \times F_{\text{price}}}{\eta_{\text{rt}}}$$
 (26)

where  $(F_{\text{slope}})$  denotes the slope of the fuel cost curve (L/kWh).

# 5.2. Load following strategy

Fig. 8 depicts the flowchart for the LF dispatch strategy used in the PV/wind/diesel/battery system [95]. This strategy operates under three main scenarios:

 PV and wind Power Equals Load Power: When the PV and wind power output matches the load demand, the system operates with the PV and wind providing all the necessary power. In this scenario, the batteries remain idle, and the generator stays off, as there is no surplus power.

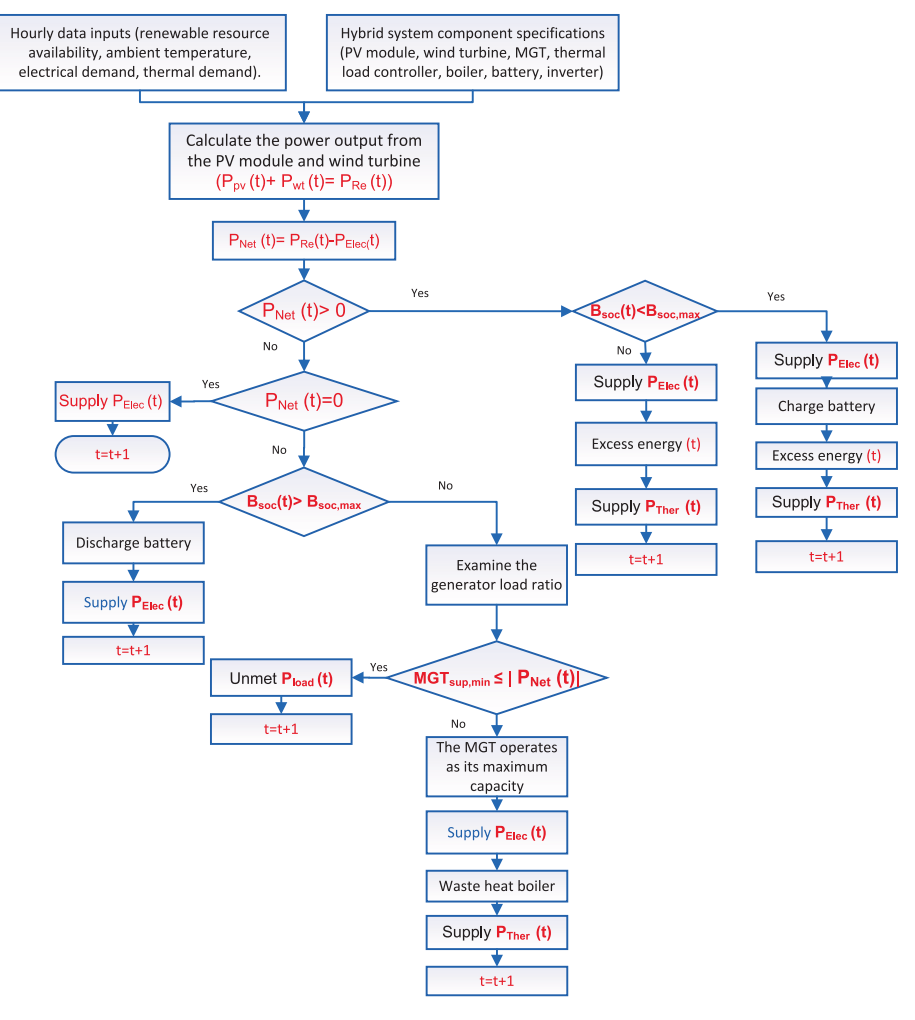


Fig. 8. Flowchart for the lf dispatch strategy used in the pv/wind/diesel/battery system.

- 2. Excess PV and wind Power: If the PV and wind output exceeds the load demand, the surplus power is first used to charge the battery if it is not fully charged. If the battery is fully charged, the excess power is curtailed. The generator remains off in this situation.
- 3. Insufficient PV and wind Power: When the PV and wind power falls short of the load demand, the following sub-cases are considered:
- Battery SOC at Minimum: If the battery SOC is at or below the minimum acceptable level, the generator operates to meet the net load (load minus PV and wind power). The generator only provides enough power to cover the net load without charging the battery. If the generator's minimum load output exceeds the net load, it can both meet the load and charge the battery with the excess PV and wind power.
- Battery SOC Above Minimum: When the SOC is above the minimum
  threshold, a comparison is made between the cost of discharging the
  battery and the cost of running the generator to meet the net load. If
  the cost of discharging the battery exceeds the cost of operating the
  generator, the generator will run to meet the load without charging
  the battery. Conversely, if discharging the battery is cheaper, the
  battery will be discharged to help meet the load.

The cost implications of these decisions are calculated as follows [95,96]:

a. Battery discharge cost

The cost of discharging the batteries is given by:

$$C_{\text{discharge}} = C_{\text{batt, wear}} \tag{27}$$

where  $(C_{\text{batt, wear}})$  represents the battery wear cost and is calculated by:

$$C_{\text{batt, wear}} = \frac{C_{\text{batt, rep}}}{N_{\text{batt}} \times Q_{\text{life}} \times \eta_{\text{rt}}}$$
 (28)

where,  $C_{\text{batt, rep}}$  is the battery replacement cost,  $N_{\text{batt}}$  is the number of batteries,  $Q_{\text{life}}$  is the single battery throughput, and  $\eta_{\text{rt}}$  is the battery round-trip efficiency.

#### b. Generator cost

The cost of operating the generator solely to meet the net load is:

$$C_{\rm gen} = \frac{F_{\rm con} \times F_{\rm price} \times L_{\rm served}}{G_{\rm output}} + \frac{C_{\rm gen, rep} \times L_{\rm served}}{G_{\rm lifetime}} + C_{\rm gen, O\&M}$$
 (29)

where  $F_{\rm con}$  is the fuel consumption rate,  $F_{\rm price}$  is the fuel price,  $L_{\rm served}$  is the total load served,  $G_{\rm output}$  is the generator output,  $G_{\rm gen, rep}$  is the generator replacement cost,  $G_{\rm lifetime}$  is the generator lifetime, and  $G_{\rm gen, O\&M}$  represents the operation and maintenance costs.

# 5.3. Novel multi-source dispatch strategy using MATLAB HOMER link

This paper presents a MATLAB-Link dispatch strategy designed to optimize the operating costs of a hybrid energy system incorporating renewable sources (solar and wind), battery storage, and diesel

generation. The MATLAB-Link interface integrates with HOMER Pro software to meet the electricity demand considering the generation of solar and wind energy [18]. The dispatch function prioritizes the utilization of renewable energy sources to minimize peak demand and reduce fuel consumption. The approach includes managing the energy output from wind and solar power, battery storage, and diesel generators to achieve cost-effective operation. The flowchart for this proposed strategy is illustrated in Fig. 9. The dispatch strategy involves several key steps and functions, each contributing to the overall optimization process. The strategy is implemented through the MATLAB Dispatch function, which coordinates the energy sources and storage systems to meet load requirements efficiently while minimizing operational costs.

#### Step 1. Initialization and parameter setup

The implementation begins by initializing necessary variables and parameters. It defines a small epsilon value to account for system errors and sets up a zero matrix to store output parameters for different dispatch scenarios. The function then configures rectifier and inverter efficiencies based on the presence of a battery system. Efficiency values are updated in the simulation parameters, and the initial states of the battery and converter systems are set to zero.

#### Step 2. Dispatching wind and solar energy

The first step in the dispatch process is to utilize available wind and solar energy. dispatch wind sources is to determine the amount of wind power available and dispatches it to meet the load. Any excess wind power is stored in the battery system if a battery is present. Similarly, the dispatch solar function is used to determine the available solar power, which is dispatched to the DC network. Excess solar power is also considered for battery charging.

#### Step 3. Battery Charging and energy storage

The strategy prioritizes the use of excess renewable energy to charge batteries. Solar energy is used first, followed by wind energy if the battery system is equipped. The charging batteries from the exceed power from the dc bus and then charging the batteries from the ac bus are employed to manage battery charging, adjusting for the efficiency of rectifiers and inverters.

#### Step 4. Generator and battery dispatch options

The function evaluates three dispatch options to meet the remaining load:

- Option 1: Discharge batteries to meet as much of the remaining load as possible, with any residual load covered by the generator. This option minimizes the marginal cost by considering battery wear and the cost of stored energy.
- Option 2: Ramp up the generator to meet the load, with excess electricity stored in the battery if the load is less than the generator's minimum output. This option balances the cost of using the generator and storing excess energy.
- Option 3: Maximize generator output to meet the load while charging the battery as much as possible. This option focuses on minimizing the marginal cost by leveraging generator output and battery storage.

Step 5. Cost Calculation and decision making

For each option, the function calculates the marginal cost, considering factors such as generator fuel cost, battery wear cost, and unmet load costs. The results of the parameters for each option, including generator power setpoint, battery power setpoint, and various operational metrics. The function selects the option with the lowest marginal

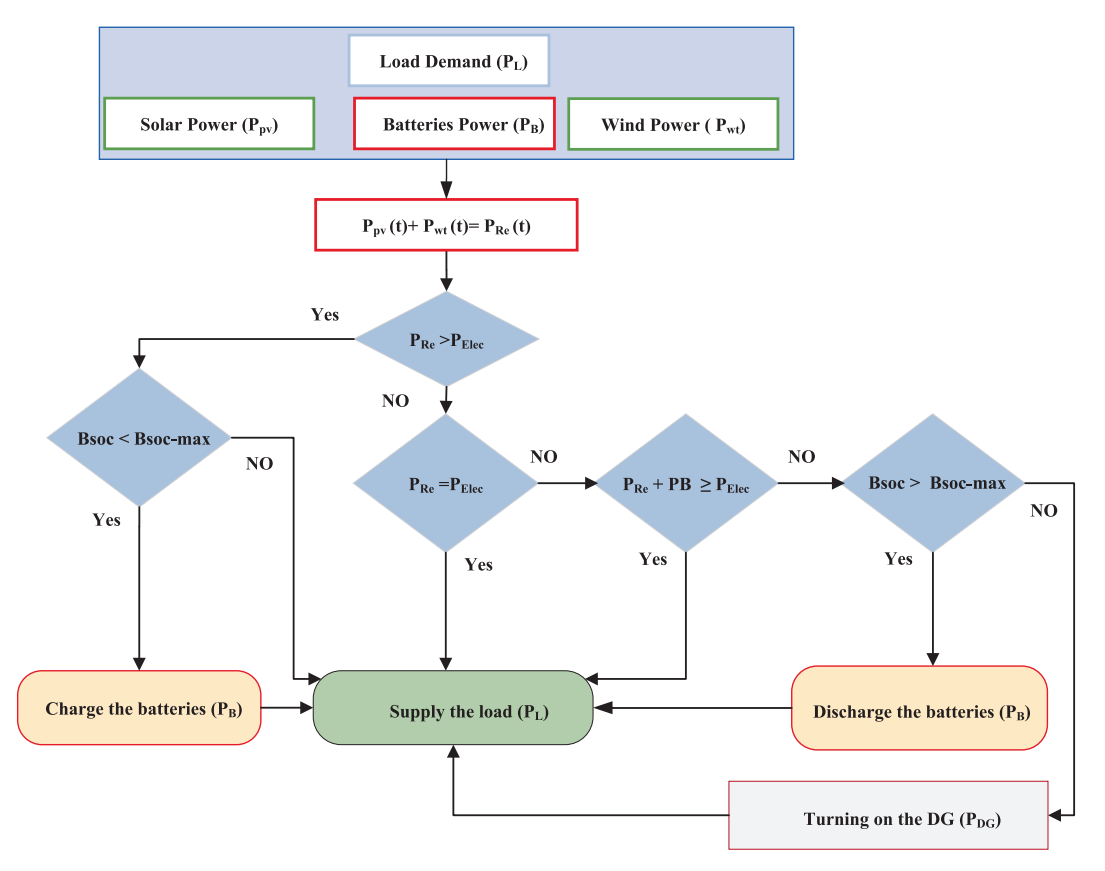


Fig. 9. Flowchart for this proposed strategy of MATLAB-Link and HOMER Pro.

cost. In case of a tie, preference is given to the option that charges the battery the most. The selected option's parameters are applied to the simulation state, optimizing the operation of the hybrid system. These steps and the accompanying flowchart outline the systematic approach for optimizing energy dispatch in hybrid systems using MATLAB-Link and HOMER Pro.

#### 5.3.1. Data transfer between HOMER and MATLAB

This section outlines the methodology for transferring data between HOMER and MATLAB, with a specific emphasis on enabling the simulation of power dispatch strategies. HOMER's dispatch algorithm determines which power resources—such as solar photovoltaic (PV), battery storage, or generators—will be dynamically allocated to meet load demands over a specified period. The data communication model facilitating this process is depicted in Fig. 10.

Fig. 10 presents the computational data transfer model between the two software platforms. To facilitate this interaction, it is essential to develop three subroutines in MATLAB: 'MatlabDispatch.m', 'MatlabStartSimulation.m', and 'MatlabEndSimulation.m'. These subroutines are instrumental in enabling the seamless exchange of data between MATLAB and HOMER. During the simulation run in HOMER, these

specifically designed to work as a controller plugin for HOMER Pro software, which is a widely used microgrid simulation tool. The dispatch strategy prioritizes renewable energy sources (wind and solar) to shave peak demand and reduce reliance on conventional generators, thereby saving fuel and reducing operational costs. It employs a hierarchical dispatch approach where renewable sources are utilized first, followed by intelligent decision-making between battery storage and generators based on marginal cost calculations. The system evaluates three different operational strategies at each timestep and selects the most economical option, considering factors such as fuel costs, battery wear, energy prices, and system constraints. This controller enables more sophisticated and economically optimized energy management than standard dispatch strategies, particularly for hybrid systems with significant renewable penetration.

### A. Objective function - Marginal cost minimization

The algorithm evaluates three dispatch options and selects the one with the lowest marginal cost per unit of load served. The marginal cost  $MC_t$  is defined as:

$$MC_{t} = \frac{C_{\text{fuel}} \cdot G_{\text{dispatched},t} + C_{\text{OM}} \cdot I_{G>0} + C_{\text{unmet}} \cdot L_{\text{unmet},t} + C_{\text{wear}} \cdot \left(B_{\text{dis},t} + B_{\text{chg},t}\right) + P_{\text{grid}} \cdot \left(B_{\text{dis},t} - B_{\text{chg},t}\right)}{L}$$

$$(30)$$

MATLAB subroutines are invoked to execute the necessary computations. Subsequently, the results, along with the workspace variables, are stored in MATLAB for further analysis.

# 5.3.2. Objective functions and constraints

The MATLAB dispatch function MatlabDispatch implements a rule-based energy management strategy for a hybrid renewable energy system. It integrates wind, solar photovoltaic (PV), battery storage, and diesel generator sources to supply electrical load demand in an economically optimal manner. The mathematical model underlying this dispatch strategy can be described using a set of equations that govern power flows, constraints, and cost minimization. The MATLAB code implements a sophisticated multi-source dispatch strategy for hybrid renewable energy systems. Its primary goal is to optimize the integration and utilization of multiple energy sources (wind, solar PV, battery storage, and conventional generators) to efficiently meet electrical demand while minimizing costs and fuel consumption. The code is

where  $I_{G>0}$  is an indicator function equal to 1 if the generator is on and  $L_{\text{unmet},t}$  can be represented as:

$$L_{\text{unmet},t} = L_t - \left( W_{\text{dispatched},t} + S_{\text{dispatched},t} + B_{\text{dis},t} + G_{\text{dispatched},t} \right)$$
(31)

Each dispatch option is evaluated using this formula, and the one with the minimum marginal cost is selected.

where  $L_t$  represents the electrical load demand at time step t.  $W_t$  and  $S_t$  denote the available wind and solar PV power, respectively, at time step t. Battery-related variables include  $B_{\mathrm{dis},t}$ , the discharge power available from the battery, and  $B_{\mathrm{chg},t}$ , the charge power to the battery, both at time step t.  $G_t$  is the generator power available at time t. The efficiencies of the inverter and rectifier are represented by  $\eta_{\mathrm{inv}}$  and  $\eta_{\mathrm{rect}}$ , respectively. Cost-related parameters include  $C_{\mathrm{fuel}}$ , the fuel cost per kilowatt-hour,  $C_{\mathrm{OM}}$ , the operation and maintenance cost per kilowatt-hour, and  $C_{\mathrm{unmet}}$ , which is the cost associated with unmet load per kilowatt-hour. Additionally,  $C_{\mathrm{wear}}$ , represents the battery wear cost per

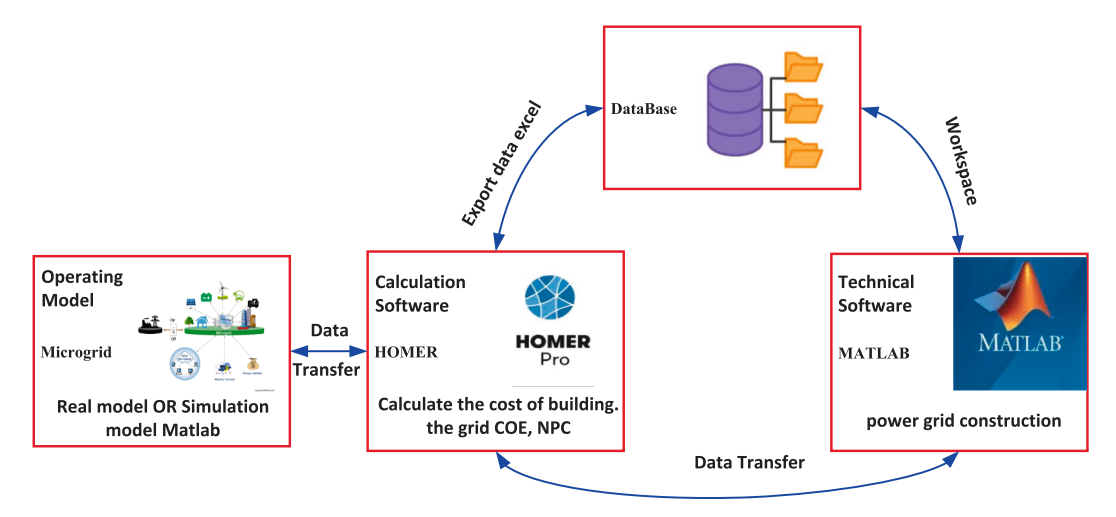


Fig. 10. Data Transfer Architecture.

kilowatt-hour. Finally,  $P_{grid}$  refers to the electricity price, which is used for evaluating the economic value of stored or unmet energy.

#### B. Constraints

Battery constraints which include the minimum and maximum state of charge (SOC) and the maximum charge/discharge power limits:

$$B_{\mathrm{chg},t} \leq B_{\mathrm{max} \setminus \mathrm{charge}}, \quad B_{\mathrm{dis},t} \leq B_{\mathrm{max} \setminus \mathrm{discharge}}$$
 (32)

Converter constraints which include the inverter and rectifier capacities:

$$P_{\text{inverter,out}} \le P_{\text{inverter,capacity}}, \quad P_{\text{rectifier,out}} \le P_{\text{rectifier,capacity}}$$
 (33)

Generator Constraints are to consider the minimum and maximum output:

$$G_{\min} \le G_{\text{dispatched},t} \le G_{\max}$$
 (34)

#### C. Decision logic - Three dispatch options

The procedure evaluates the following three dispatch strategies:

Option 1: Discharge Battery First.

The dispatch strategy prioritizes battery discharge before using the generator.

$$MC_{1} = \frac{C_{\text{fuel}} \cdot G_{\text{dispatched},t} + C_{\text{wear}} \cdot B_{\text{dis},t} + C_{\text{unmet}} \cdot L_{\text{unmet},t}}{L_{t}}$$
(35)

Option 2: Generator Follows Load

The dispatch strategy uses the generator to meet the net load and stores excess electricity in the battery when possible.

$$MC_{2} = \frac{C_{\text{fuel}} \cdot G_{\text{dispatched},t} + C_{\text{wear}} \cdot B_{\text{chg},t} - P_{\text{grid}} \cdot B_{\text{chg},t} + C_{\text{unmet}} \cdot L_{\text{unmet},t}}{L_{t}}$$
(36)

Option 3: Maximize Generator Output and Charge Battery

The dispatch strategy ramps up the generator fully and charges the battery whenever possible.

$$MC_{3} = \frac{C_{\text{fuel}} \cdot G_{\text{dispatched},t} + C_{\text{wear}} \cdot B_{\text{chg},t} - P_{\text{grid}} \cdot B_{\text{chg},t}}{L_{t}}$$
(37)

The algorithm selects the option with the lowest  $MC_t$ . If two options have equal cost, the one that results in higher battery charging is chosen.

D. Final decision rule

Selected Option = 
$$\arg\min_{i=1} MC_i$$
 (38)

If multiple options yield the same marginal cost:

Selected Option = 
$$\max(B_{\text{chg},t})$$
 (39)

The mathematical model is the core logic of the 'MatlabDispatch' function. It balances renewable energy utilization, battery operation, and generator use under economic and technical constraints. The optimization is based on minimizing the marginal cost of supplying electricity while ensuring reliability and efficiency in a hybrid microgrid environment.

#### 6. Results

This section details the results of the technical, economic, and environmental evaluations conducted for the Sharurah case study using HOMER. The analysis compares the efficacy of three dispatch strategies: CC, LF, and a proposed MATLAB-linked strategy. The study aims to optimize a hybrid PV/Diesel/Battery system tailored to the specific conditions of Sharurah, KSA.

#### 6.1. Baseline standalone diesel system

During the baseline scenario, a diesel generator system that is independent was evaluated in terms of performance. The simulation results show that the system is dependent on continuous diesel generator operation to satisfy full load demand, resulting in significant fuel consumption and increased operational costs. The estimated NPC for this configuration is \$47.782 million, and the LCOE is \$0.201/kWh. This scenario has a significant environmental impact as it does not incorporate renewable energy sources, resulting in CO2 emissions reaching 12,889,344 kg/year. The system's heavy reliance on diesel makes it crucial to incorporate renewable energy sources to enhance sustainability and reduce emissions.

#### 6.2. Optimized hybrid PV/wind/diesel/battery system

The optimization scenario improves efficiency and reduces cost through better hybrid system design. It increases renewable capacity, optimizes storage, and uses advanced dispatch strategies. Simulations in HOMER identified five configurations: Base Case, Cycle Charging, Load Following, and two MATLAB-linked options (with and without a diesel generator). The selection was based on the Net Present Cost (NPC).

The Base Case relies entirely on a 4,300 kW generator, with no renewables or storage. This leads to high fuel use, emissions, and operating cost. Cycle Charging adds 5,450 kW PV, 5,476 kW wind, 57 battery strings, and a 3,058 kW converter. Load Following increases PV to 7,562 kW, uses 5,361 kW wind, 32 batteries, and a 3,573 kW converter—balancing storage and renewable input. The MATLAB-linked case without a generator shifts toward full renewable integration: 14,091 kW PV, 26 kW wind, only 15 battery strings, and a 5,823 kW converter. The version with the generator uses 5,533 kW PV, 71 kW wind, 47 battery strings, and a 3,106 kW converter. Both versions reduce emissions and costs, with the no-generator scenario being the most sustainable and efficient.

Table 4 summarizes financial metrics for the Base Case and four optimized scenarios: Cycle Charging, Load Following, and Pro MATLAB Link (with and without diesel generator). The Base Case has the highest total NPC at \$47.78 M, driven by high operating (\$14.6 M) and resource costs (\$25.5 M). Although its CAPEX is low (\$946,000), long-term expenses make it the least efficient option. Cycle Charging and Load Following lower NPC to \$35.81 M and \$33.67 M, respectively, through renewable integration. These options increase CAPEX (\$19.4 M and \$17.6 M) but cut fuel and operating costs significantly. Pro MATLAB Link without DG yields the lowest NPC (\$16.4 M) and shortest payback period (3.08 years). It also has the lowest operating cost (\$2.26 M) and no resource cost, thanks to full renewable reliance. Its LCOE is competitive at \$0.14/kWh. The MATLAB Link with DG option reaches \$34.45 M NPC, higher than the no-DG variant due to added generator fuel cost. All optimized systems outperform the Base Case in LCOE, with values ranging from \$0.14 to \$0.15/kWh, compared to \$0.201/kWh. The comparison confirms the Pro MATLAB Link system offers the best return on investment and cost efficiency.

**Table 4**The financial metrics for the Base Case and four RES configurations.

Name	Base Case	HOMER Cycle Charging	HOMER Load Following	HOMER Pro MATLA	HOMER Pro MATLAB Link	
				Without DG	With DG	
Total NPC (\$)	47,781,820.00	35,810,180.00	33,674,350.00	16,395,890.00	34,454,062.27	
LCOE (\$/kWh)	0.201	0.15	0.14	0.14	0.1447	
Capital	\$946,000	\$19.4 M	\$17.6 M	\$13.9 M	\$12.2 M	
Operating	\$14.6 M	\$5.00 M	\$5.83 M	\$2.26 M	\$9.19 M	
Replacement	\$6.86 M	\$4.00 M	\$4.34 M	\$674,562	\$4.10 M	
Salvage	-\$91,782	-\$1.01 M	-\$558,271	-\$445,364	-\$638,988	
Resource	\$25.5 M	\$8.43 M	\$6.44 M	\$0.00	\$9.58 M	
Simple payback period (Year)	N/A	7.22	6.44	3.08	7.8	

Table 5
The performance of four microgrid systems—Base System, HOMER Cycle Charging, HOMER Load Following, and HOMER Pro MATLAB Link.

	Base System	HOMER Cycle Charging	HOMER Load Following	HOMER Pro MATL	AB Link
				Without DG	With DG
Net Present Cost	\$47.8 M	\$35.8 M	\$33.7 M	\$16.4 M	\$34.5 M
CAPEX	\$946,000	\$19.4 M	\$17.6 M	\$13.9 M	\$12.2 M
OPEX	\$3.62 M	\$1.27 M	\$1.24 M	\$192,426	\$1.72 M
LCOE (per kWh)	\$0.20	\$0.15	\$0.14	\$0.14	\$0.145
CO2 Emitted (kg/yr)	12,889,340	4,266,308	3,257,748	0	6,466,112
Fuel Consumption (L/yr)	4,924,080	1,629,846	1,244,548	0	2,470,230

Table 5 compares the economic and environmental performance of four microgrid systems: Base System, HOMER Cycle Charging, HOMER Load Following, and HOMER Pro MATLAB Link (with and without diesel generator). The Base System shows the highest NPC at \$47.8 M, driven by high fuel consumption (4.92 million L/yr) and CO<sub>2</sub> emissions (12.89 million kg/yr). Despite a low CAPEX (\$946,000), its OPEX (\$3.62 M) and LCOE (\$0.20/kWh) highlight its financial and environmental inefficiency. Cycle Charging and Load Following cut fuel use and emissions significantly. NPC drops to \$35.8 M and \$33.7 M, with fuel usage reduced to 1.63 M and 1.24 M L/yr, respectively. CO2 emissions fall to 4.27 M and 3.26 M kg/yr. Though their CAPEX is higher (\$19.4 M and \$17.6 M), both options achieve lower OPEX and LCOE (\$0.15 and \$0.14/kWh), offering more balanced performance. The HOMER Pro MATLAB Link (without DG) offers the lowest NPC at \$16.4 M, with zero fuel consumption and CO<sub>2</sub> emissions. Its OPEX is minimal (\$192,426), and CAPEX remains moderate at \$13.9 M. It matches the best LCOE value at \$0.14/kWh. This system maximizes renewable integration and optimization, achieving full decarbonization. The Pro MATLAB Link with DG configuration reintroduces emissions and fuel use, raising NPC to \$34.5 M, though it still improves upon the Base Case. Across all metrics, the MATLAB-linked strategy without DG achieves the best performance. It delivers the lowest total cost, the shortest payback, zero

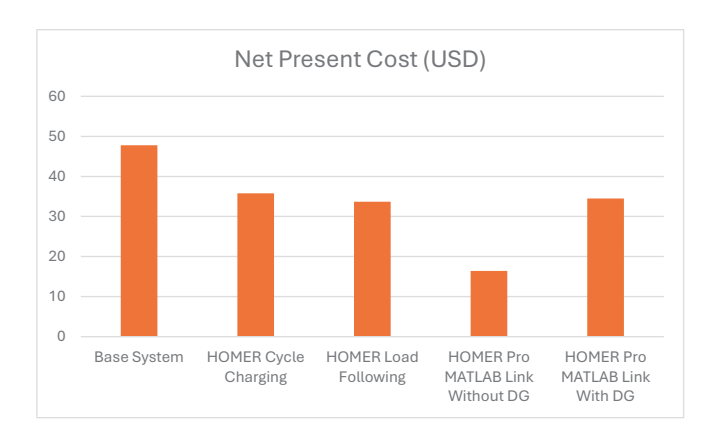


Fig. 11. Comparison validation of NPC among the three methods with the base case.

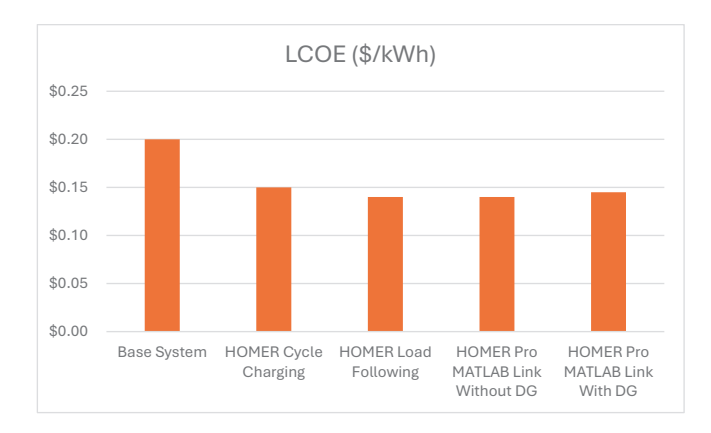


Fig. 12. Comparison validation of LCOE among the three methods with the base case.

emissions, and full renewable operation The results have been visualized in Figs. 11 and 12.

#### 6.3. Economic analysis

The economic analysis, conducted using HOMER software, evaluated five hybrid energy system (HES) configurations: a base case and four optimized scenarios (Cycle Charging, Load Following, MATLAB Link without DG, and MATLAB Link with DG). Each was assessed for capital, operating, replacement, salvage, and resource costs. Table 6 summarizes the financial breakdown. The base case, dependent solely on a diesel genset, has the highest total cost at \$47.8 M, due to high fuel, O&M, and replacement costs. No renewables are present. The Cycle Charging strategy reduces total cost to \$35.8 M. It includes investments in PV (\$3.49 M), wind (\$7.41 M), and batteries, leading to lower fuel and O&M expenses. Load Following further improves cost-efficiency, reaching \$33.7 M total. While it allocates more to PV (\$4.84 M) and batteries, wind investment is lower than Cycle Charging, resulting in balanced savings across all cost categories. The MATLAB Link without DG case achieves the lowest cost, \$16.4 M, with a high PV share (\$9.02 M) and minimal wind (\$1.95 M). Eliminating diesel use significantly cuts O&M and fuel costs. The MATLAB Link with DG adds a genset for

Table 6
Financial breakdown for four different microgrid scenarios, including a base case and three optimized configurations.

	Name	Capital	Operating	Replacement	Salvage	Resource	Total
Base Case	Autosize Genset	0.946 M	\$14.6 M	\$6.86 M	-0.091782 M	\$25.5 M	\$47.8 M
	Converter	0	0	0	0	0	0
	Eocycle EOX M-21 [100 kW]	0	0	0	0	0	0
	PV	0	0	0	0	0	0
	Surrette 8 CS 25P	0	0	0	0	0	0
	System	0.946 M	\$14.6 M	\$6.86 M	-0.091782 M	\$25.5 M	\$47.8 M
HOMER Cycle Charging	Autosize Genset	0.946 M	\$3.30 M	\$1.27 M	-0.159768 M	\$8.43 M	\$13.8 M
	Converter	\$1.53 M	0.217436 M	0.341233 M	-0.192306 M	\$0.00	\$1.90 M
	Eocycle EOX M-21 [100 kW]	\$7.41 M	0.073687 M	\$0.00	-0.295854 M	\$0.00	\$7.19 M
	PV	\$3.49 M	0.704590 M	\$0.00	\$0.00	\$0.00	\$4.19 M
	Surrette 8 CS 25P	\$6.02 M	0.707911 M	\$2.39 M	-0.364727 M	\$0.00	\$8.75 M
	System	\$19.4 M	\$5.00 M	\$4.00 M	-\$1.01 M	\$8.43 M	\$35.8 M
HOMER Load Following	Autosize Genset	0.946 M	\$3.87 M	\$1.42 M	-0.030972 M	\$6.44 M	\$12.6 M
	Converter	\$1.79 M	0.254052 M	\$398,695	-0.224690 M	\$0.00	\$2.21 M
	Eocycle EOX M-21 [100 kW]	\$4.16 M	0.041368 M	\$0.00	-0.166093 M	\$0.00	\$4.04 M
	PV	\$4.84 M	0.977538 M	\$0.00	\$0.00	\$0.00	\$5.82 M
	Surrette 8 CS 25P	\$5.90 M	0.693044 M	\$2.52 M	-0.136515 M	\$0.00	\$8.97 M
	System	\$17.6 M	\$5.83 M	\$4.34 M	-0.558271 M	\$6.44 M	\$33.7 M
HOMER Pro MATLAB Link without DG	Autosize Genset	0	0	0	0	0	0
	Converter	\$2.91 M	0.413995 M	0.649701 M	-0.366148 M	\$0.00	\$3.61 M
	Eocycle EOX M-21 [100 kW]	\$1.95 M	0.019391 M	\$0.00	-0.77856 M	\$0.00	\$1.89 M
	PV	\$9.02 M	\$1.82 M	\$0.00	\$0.00	\$0.00	\$10.8 M
	Surrette 8 CS 25P	0.028600 M	0.003361 M	0.024861 M	-0.001360 M	\$0.00	0.055463 M
	System	\$13.9 M	\$2.26 M	0.674562 M	-0.445364 M	\$0.00	\$16.4 M
HOMER Pro MATLAB Link with DG	Autosize Genset	\$946,000	\$8.18 M	\$3.73 M	-\$186,963	\$9.58 M	\$22.2 M
	Converter	\$1.55 M	\$220,843	\$346,579	-\$195,319	\$0.00	\$1.93 M
	Eocycle EOX M-21 [100 kW]	\$6.11 M	\$60,759	\$0.00	-\$243,950	\$0.00	\$5.93 M
	PV	\$3.54 M	\$715,294	\$0.00	\$0.00	\$0.00	\$4.26 M
	Surrette 8 CS 25P	\$78,100	\$9,179	\$22,635	$-\$12,\!756$	\$0.00	\$97,157
	System	\$12.2 M	\$9.19 M	\$4.10 M	-\$638,988	\$9.58 M	\$34.5 M

Table 7
Comparison for PV Performance of dispatch strategies: Base System, HOMER Cycle Charging, HOMER Load Following, and HOMER Pro MATLAB Link (with/without DG).

Quantity	Units	Base System	HOMER Cycle Charging	HOMER Load Following	HOMER Pro MATLAB Link	
					Without DG	With DG
Minimum Output	kW	0	0	0	0	0
Maximum Output	kW	0	5,225	7,249	13,509	5,386
PV Penetration	%	0	57.6	79.9	149	58.5
Hours of Operation	hrs/yr	0	4,320	4,320	4,320	4,320
Levelized Cost	\$/kWh	0	0.0306	0.0306	0.0306	0.0306
Rated Capacity	kW	0	5,450	7,562	14,091	5,533
Mean Output	kW	0	1,211	1,679	3,130	1,229
Mean Output	kWh/d	0	29,053	40,307	75,113	29,494
Capacity Factor	%	0	22.2	22.2	22.2	22.2
Total Production	kWh/yr	0	10,604,283	14,712,215	27,416,318	10,765,47

 Table 8

 Wind turbine performance across configurations.

Quantity	Units	Base System	HOMER Cycle Charging	HOMER Load Following	HOMER Pro MATLAB Link	
					Without DG	With DG
Minimum Output	kW	0	0	0	0	0
Maximum Output	kW	0	2,989	1,678	787	2,464
Wind Penetration	%	0	41.7	23.4	11	34.4
Hours of Operation	hrs/yr	0	4,047	4,047	4,047	4,047
Levelized Cost	\$/kWh	0	0.0723	0.0723	0.0723	0.0723
Total Rated Capacity	kW	0	5,700	3,200	1,500	4,700
Mean Output	kW	0	877	493	231	723
Capacity Factor	%	0	15.4	15.4	15.4	15.4
Total Production	kWh/yr	0	7,685,290	4,314,549	2,022,445	6,336,993

backup. Its total cost is \$34.5 M—still lower than HOMER's default strategies. The PV, wind, and converter investments remain balanced, but genset-related costs raise operating expenses. The results highlight that the MATLAB-linked optimization delivers superior cost performance, especially when diesel use is minimized. It achieves the lowest LCOE by reducing fuel dependency and enhancing renewable integration (Table 7).

#### 6.4. Electrical analysis

The Base System, which relies solely on conventional power generation without renewable integration, shows no PV output, penetration, or energy production. In contrast, the optimized HOMER configurations demonstrate significant improvements through solar PV integration. The HOMER Cycle Charging strategy achieves a maximum output of 5,225 kW with 57.6 % PV penetration, producing 10.6 million kWh annually at a levelized cost of \$0.0306/kWh. The HOMER Load Following strategy further enhances performance, reaching 7,249 kW maximum output and 79.9 % PV penetration, while maintaining the same cost efficiency and generating 14.7 million kWh annually.

The HOMER Pro MATLAB Link (Without DG) system outperforms both, delivering a remarkable 13,509 kW maximum output and 149 % PV penetration, with annual production soaring to 27.4 million kWh—all while sustaining a 22.2 % capacity factor and the same competitive LCOE. Meanwhile, the HOMER Pro MATLAB Link (With DG) configuration balances PV and conventional generation, achieving 5,386 kW maximum output and 58.5 % PV penetration, with annual production of 10.8 million kWh. All HOMER systems operate for 4,320 h per year, proving the reliability and cost-effectiveness of renewable integration. The MATLAB-linked dispatch strategy stands out by maximizing solar utilization, significantly reducing fossil fuel dependence while maintaining economic and operational efficiency. This highlights the critical role of advanced optimization in scaling renewable energy systems.

Table 8 provides insight into the performance of the Eocycle EOX M—21 100 kW wind turbines in the Base System and three HOMER-optimized configurations (Cycle Charging, Load Following, and Pro MATLAB Link). The Base System shows no wind energy integration, while HOMER-optimized configurations demonstrate varying levels of wind power utilization. The Cycle Charging strategy leads with 5,700 kW rated capacity, achieving 2,989 kW max output and 41.7 % wind penetration, producing 7.68 million kWh annually. Load Following shows moderate integration (3,200 kW capacity, 23.4 % penetration), while Pro MATLAB Link minimizes wind reliance (1,500 kW capacity, 11 % penetration). All configurations maintain a 15.4 % capacity factor, 4,047 annual operating hours and \$0.0723/kWh LCOE. The results show Cycle Charging's strong wind dependence versus Pro MATLAB Link's preference for other renewables, particularly solar, while maintaining consistent cost efficiency.

Table 9 summarizes the converter performance for the Base System and four HOMER configurations. The Base System includes no converter, so all metrics are zero. In contrast, the HOMER configurations use

converters to manage power flow from renewables and storage. Load Following runs the converter the most (7,012 hrs/yr), outputs the most energy (9.65 million kWh/yr), and shows the highest losses (507,933 kWh/yr). Its 3,573 kW converter achieves a 30.8 % capacity factor. Cycle Charging operates for 5394 hrs/yr, with 7.63 million kWh/yr output and 401,695 kWh/yr losses. It uses a 3,058 kW converter with 28.5 % capacity factor. MATLAB Link with DG runs for 3,683 hrs/yr with 4.3 million kWh/yr output and 226,325 kWh/yr losses. Its 3,106 kW converter reaches a 15.8 % capacity factor. MATLAB Link Without DG has the largest converter (5,823 kW) but a lower capacity factor of 13.6 %. It operates 5,866 hrs/yr, outputs 6.95 million kWh/yr, and has the lowest losses at 365,620 kWh/yr. Overall, Load Following achieves the highest utilization, while MATLAB-based models prioritize flexibility and efficiency. Figs. 13 and 14 show monthly power output with and without the DG under the MATLAB Link setup.

#### 6.5. Energy storage

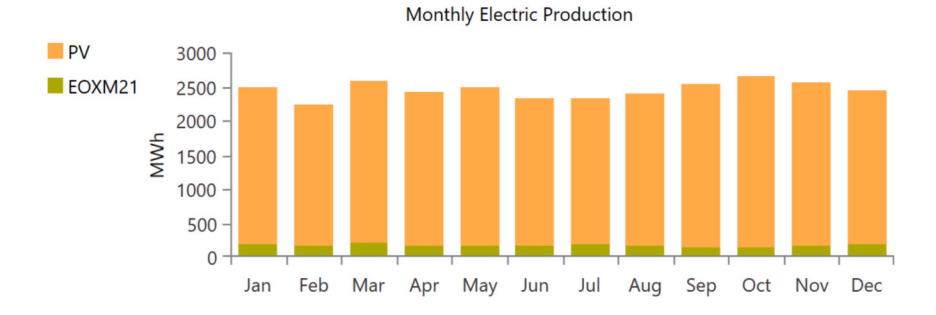
Energy storage is vital in HESs to store excess power and supply it when needed. Battery sizing directly affects system performance and cost. Battery lifetime depends on annual energy throughput (kWh/year); more charge/discharge cycles reduce lifespan. Table 9 summarizes Surrette 8 CS 25P battery use across five configurations. The base System has no storage; all values are zero. Moreover, the cycle Charging and Load Following use over 5,000 batteries each in single-string setups. Both have high throughput (5.5-6 million kWh/yr) and large losses (over 1 million kWh/yr) due to frequent cycling. The MATLAB Link Without DG uses only 26 batteries in parallel strings. Input/output is much lower (42,759/34,339 kWh/yr), with minimal losses (8,567 kWh/ yr), showing efficient usage. Autonomy is \sim 14 hrs for Cycle Charging and Load Following, and just 0.0704 hrs (4.2 min) for MATLAB Link. The lifetimes are 14.5 yrs (Cycle Charging), 13.2 yrs (Load Following), and 9 yrs (MATLAB Link). The degradation cost is fixed at \\$0.0842/ kWh for all. Fig. 15 shows the state of charge for MATLAB Link. The results confirm its minimal battery reliance compared to the other setups (Fig. 16).

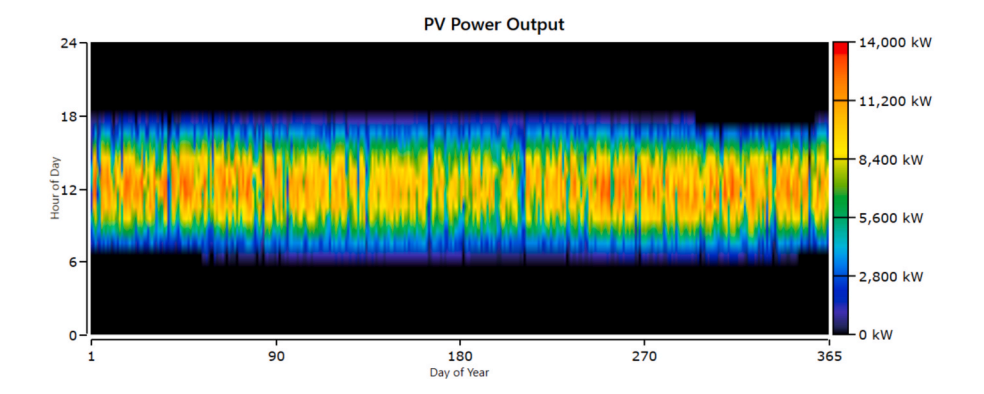
#### 6.5.1. Impact on battery life

Battery life in microgrids depends on how renewable energy is integrated and how the system is configured. The Base System uses only diesel. It includes no batteries, so battery life is not relevant. The HOMER Cycle Charging configuration uses 5,476 strings. Annual throughput is around 5 million kWh, with 1.12 million kWh lost in storage. Batteries cycle moderately. The expected life is 14.5 years due to balanced charge–discharge patterns. The HOMER Load Following system has 5,361 strings, with a slightly higher throughput of 5.39 million kWh and 1.20 million kWh in losses. More frequent cycling reduces battery life to 13.2 years. The HOMER Pro MATLAB Link uses only 26 strings, relying mostly on real-time solar and wind. Throughput is much lower at 38,392 kWh/yr, with losses of 8,567 kWh/yr. Fewer cycles occur, but each use is more intense. The smaller battery bank results in a shorter life of 8.99 years. Battery life improves with proper

**Table 9**The converter performance across configurations.

Quantity	Units	Base System	<b>HOMER Cycle Charging</b>	HOMER Load Following	HOMER Pro MATLAB Link	
					Without DG	With DG
Hours of Operation	hrs/yr	0	5,394	7,012	5,866	3,683
Energy Out	kWh/yr	0	7,632,210	9,650,727	6,946,788	4,300,167
Energy In	kWh/yr	0	8,033,905	#	7,312,408	4,526,491
Losses	kWh/yr	0	401,695	507,933	365,620	226,325
Capacity	kW	0	3,058	3,573	5,823	3,106
Mean Output	kW	0	871	1,102	793	491
Minimum Output	kW	0	0	0	0	0
Maximum Output	kW	0	2,777	3,248	3,337	3,106
Capacity Factor	%	0	28.5	30.8	13.6	15.8





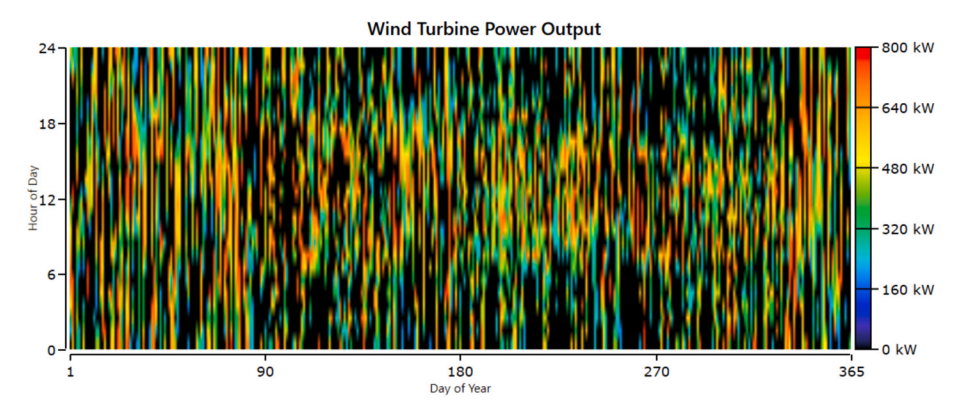


Fig. 13. A) monthly electrical production, b) pv output production and c) the wind turbine power production using homer pro matlab link without dg.

sizing and balanced cycling. High renewable penetration can extend or reduce life depending on system design and storage stress levels.

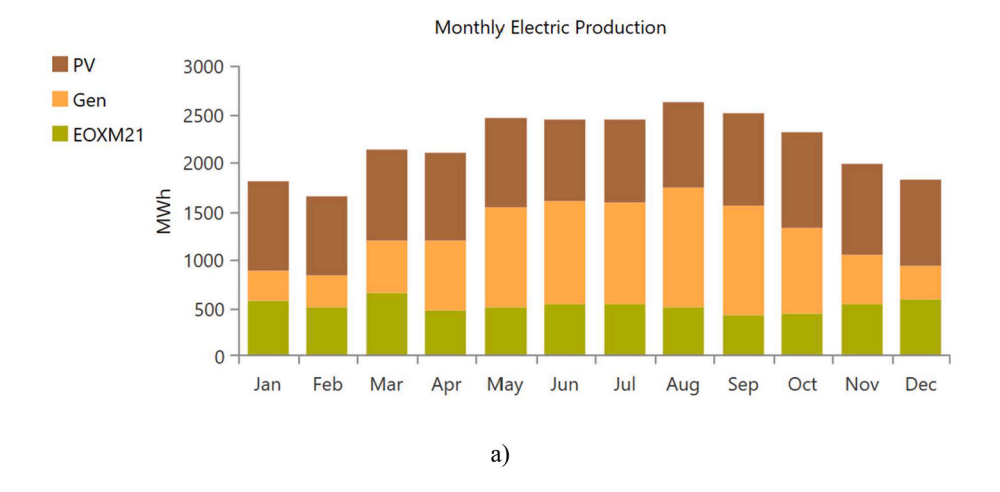
# 6.5.2. Impact on long-term costs

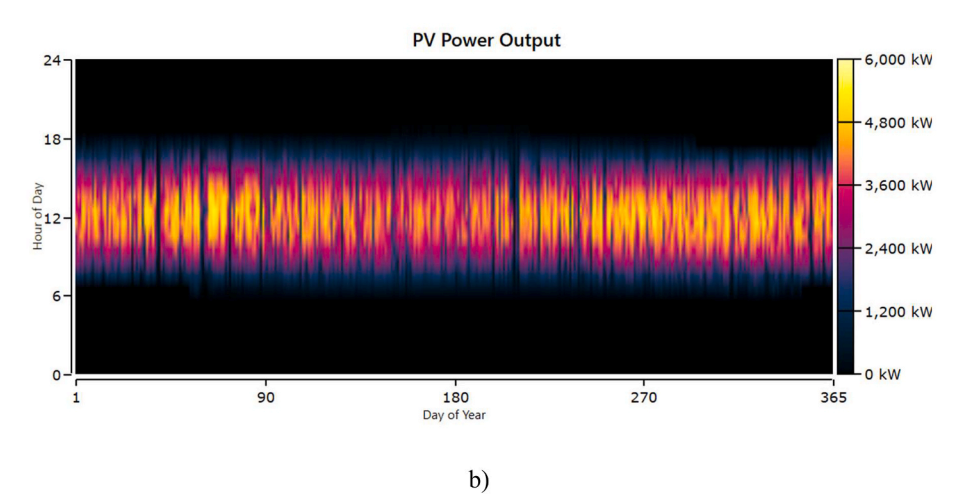
The integration of renewables and battery storage directly affects the long-term cost of microgrid systems. Table 10 compares five configurations: Base System, HOMER Cycle Charging, HOMER Load Following, HOMER Pro MATLAB Link Without DG, and With DG. The base system uses only a diesel generator. No batteries. Highest cost: NPC \$47.8 M, with 4.92 M liters/year fuel consumption and high OPEX due to fuel and maintenance. Such system is a not sustainable. HOMER Cycle Charging combines renewables and 5,476 battery strings. NPC drops to \$35.8 M. Diesel use is cut significantly. Battery throughput is  $\sim 5.0$  M kWh/year. Storage wear cost is \$0.0842/kWh. Battery life: 14.5 years. The HOMER LF is a similar setup with 5,361 battery strings. Better load matching reduces diesel use further. NPC is \$33.7 M. Higher throughput (5.39 M kWh/year) slightly shortens battery life to 13.2 years. On the other hand, the HOMER Pro MATLAB Link Without DG is fully renewable with only 26 battery strings. Very low energy throughput (38,392 kWh/year). NPC drops sharply to \$16.4 M. Battery life is 8.99 years due to high cycling intensity relative to capacity. Moreover, the HOMER Pro MATLAB Link With DG is a hybrid system with minimal DG backup. Uses 71 battery strings. Lower throughput (10,503 kWh/year) but optimized cycling gives longest battery life: 20 years. Maintains low OPEX with moderate CAPEX. The HOMER Pro MATLAB Link configurations offer the lowest long-term costs. The system without DG achieves full fuel independence. The version with DG balances cost, reliability, and battery longevity. Fig. 15 shows the system payback (Table 11).

## 6.6. Environmental analysis

# 6.6.1. Diesel consumption Statistics

The data on diesel consumption demonstrates the environmental impact of fuel usage across the Base System and the HOMER-optimized configurations— CC, LF, and MATLAB Link (ML), as in table 11. The Base System uses the most fuel, with 4.92 million liters per year. HOMER Cycle Charging cuts this to 1.63 million liters, while HOMER Load Following reduces it further to 1.24 million liters. The HOMER Pro MATLAB Link without DG consumes no diesel at all. With limited generator use, the HOMER Pro MATLAB Link with DG uses 2.47 million liters per year. These results confirm that renewable-integrated systems, especially those without DG, significantly reduce diesel dependency.





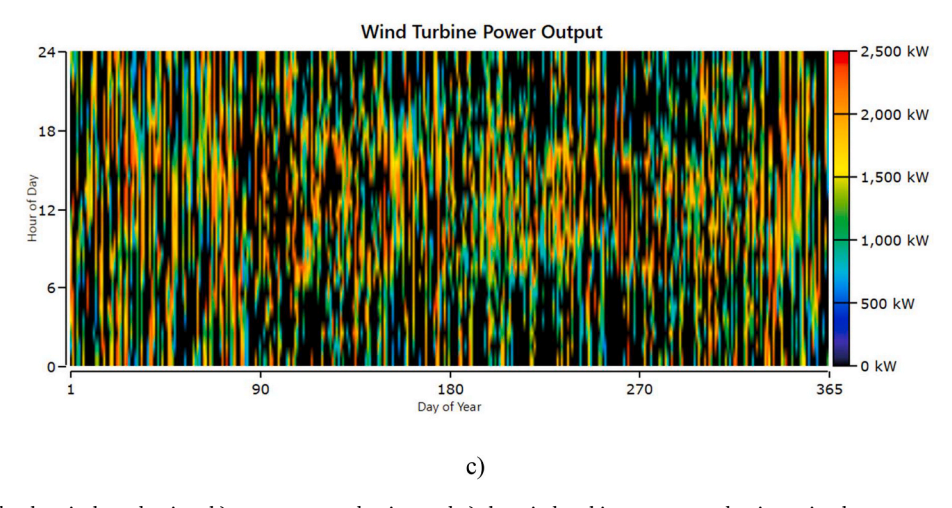


Fig. 14. A) monthly electrical production, b) pv output production and c) the wind turbine power production using homer pro matlab link with dg.

# 6.6.2. Emissions

Table 12 highlights the emissions profile of each system configuration. The Base System, which relies entirely on diesel, produces the highest emissions, with 12.89 million kg of  $CO_2$  per year, along with significant levels of CO,  $NO_x$ , UHC, PM, and  $SO_2$ . The HOMER Cycle Charging system reduces  $CO_2$  emissions to 4.27 million kg/yr, cutting other pollutants by similar proportions due to lower diesel usage. The HOMER Load Following system performs even better, reducing  $CO_2$  to 3.26 million kg/yr with further decreases in all other emissions. The HOMER Pro MATLAB Link Without DG achieves zero emissions, as it

runs entirely on renewable energy. Meanwhile, the HOMER Pro MATLAB Link With DG produces moderate emissions—6.47 million kg of  $\rm CO_2$  annually—due to limited generator use. These results confirm that renewable-based configurations, especially those without diesel generators, offer significant environmental benefits by minimizing emissions and reducing reliance on fossil fuels.

# 6.7. Sensitivity Analysis: Impact of diesel price on system performance

A sensitivity analysis has been conducted to evaluate how varying

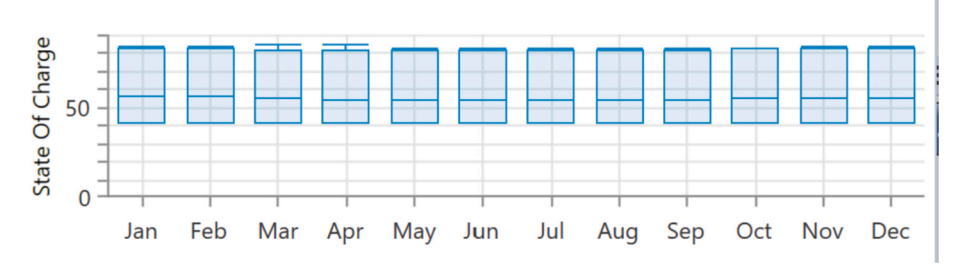
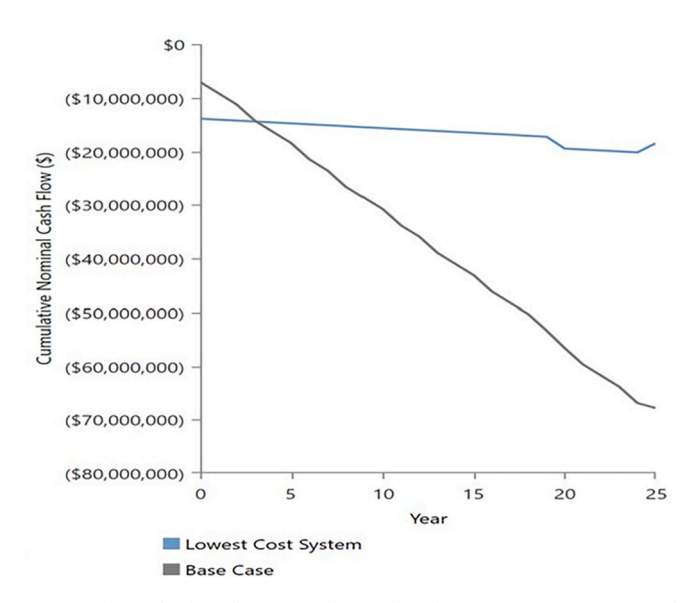


Fig. 15. The state of charge during the year from Pro MATLAB Link without DG in the system.



 $\begin{tabular}{ll} \textbf{Fig. 16.} & \textbf{The payback of the system designed with HOMER Pro MATLAB Link without DG.} \end{tabular}$ 

diesel prices affect the Net Present Cost (NPC) and capacity shortage of the hybrid energy system (HES). The scenarios have been analyzed under three diesel price points: \$0.30/L, \$0.40/L, and \$0.60/L. The analysis considered the effect of diesel price changes on NPC relative to converter, battery, and generator capacities as shown in Figs. 17, 18 and 19. At a diesel price of \$0.30/L, NPC values showed moderate sensitivity to converter and battery sizing. Systems with larger battery capacities slightly reduced NPC due to enhanced load shifting and fewer generator operating hours. However, diesel generator use remained cost-effective enough to sustain a balanced hybrid configuration. Increasing the diesel price to \$0.40/L led to a more noticeable reduction in NPC for configurations with higher renewable integration and larger battery or converter capacity. The reliance on diesel generators became less economically favorable, highlighting the cost advantage of storage and renewable energy sources in offsetting operational costs. At the highest price point of \$0.60/L, systems with minimal diesel dependence—such as the HOMER Pro MATLAB Link Without DG-became significantly more attractive. NPC increased steeply for configurations with higher generator usage, especially where battery and converter capacities were limited. Conversely, configurations with greater storage and inverter sizing effectively suppressed NPC growth, making them more economically resilient to diesel price volatility. Capacity shortage sensitivity followed a similar trend. At lower diesel prices, systems with lower battery capacities showed acceptable performance. As prices rose, the

Table 10
Performance of the storage system for the designed configurations.

Quantity	Units	Base System	HOMER Cycle Charging	HOMER Load Following	HOMER Pro MA	ΓLAB Link
					Without DG	With DG
Batteries	qty.	0	5,476	5,361	26	71.0
String Size	batteries	0	1	1	1	1.00
Strings in Parallel	strings	0	5,476	5,361	26	71.0
Bus Voltage	V	0	8	8	8	8.00
Average Energy Cost	\$/kWh	0	0.028	0	0	0
Energy In	kWh/yr	0	5,592,016	6,015,350	42,759	11,569
Energy Out	kWh/yr	0	4,477,104	4,820,211	34,339	9,394
Storage Depletion	kWh/yr	0	3,904	8,868	148	155
Losses	kWh/yr	0	1,118,815	1,204,006	8,567	2,330
Annual Throughput	kWh/yr	0	5,005,555	5,389,160	38,392	10,503
Autonomy	hr	0	14.8	14.5	0.0704	0.192
Storage Wear Cost	\$/kWh	0	0.0842	0.0842	0.0842	0.0842
Nominal Capacity	kWh	0	51,953	50,862	247	674
Usable Nominal Capacity	kWh	0	31,172	30,517	148	404
Lifetime Throughput	kWh	0	72,671,996	71,145,831	345,046	210,066
Expected Life	yr	0	14.5	13.2	8.99	20.0

 Table 11

 Diesel Consumption Statistics for the designed configurations.

	U	· ·					
Quantity	Units	Base case	CC	LF	HOMER Pro MATLA	HOMER Pro MATLAB Link	
					Without DG	With DG	
Total fuel consumed	L	4,924,080	1,629,845	1,244,548	0	2,470,230	
Avg fuel per day	L/day	13,491	4,465	3,410	0	6,768	
Avg fuel per hour	L/hour	562	186	142	0	282	

**Table 12** Emissions for the designed configurations.

Pollutant	Unit	Base case	CC	LF	HOMER Pro MATLAB Link	
					Without DG	With DG
Carbon Dioxide	kg/yr	12,889,344	4,266,308	3,257,748	0	6,466,111
Carbon Monoxide	kg/yr	81,247	26,892	20,535	0	40,759
Unburned Hydrocarbons	kg/yr	3,545	1,173	896	0	1,779
Particulate Matter	kg/yr	492	163	124	0	247
Sulfur Dioxide	kg/yr	26,039	8,619	6,581	0	13,063
Nitrogen Oxides	kg/yr	76,323	25,263	19,290	0	38,289

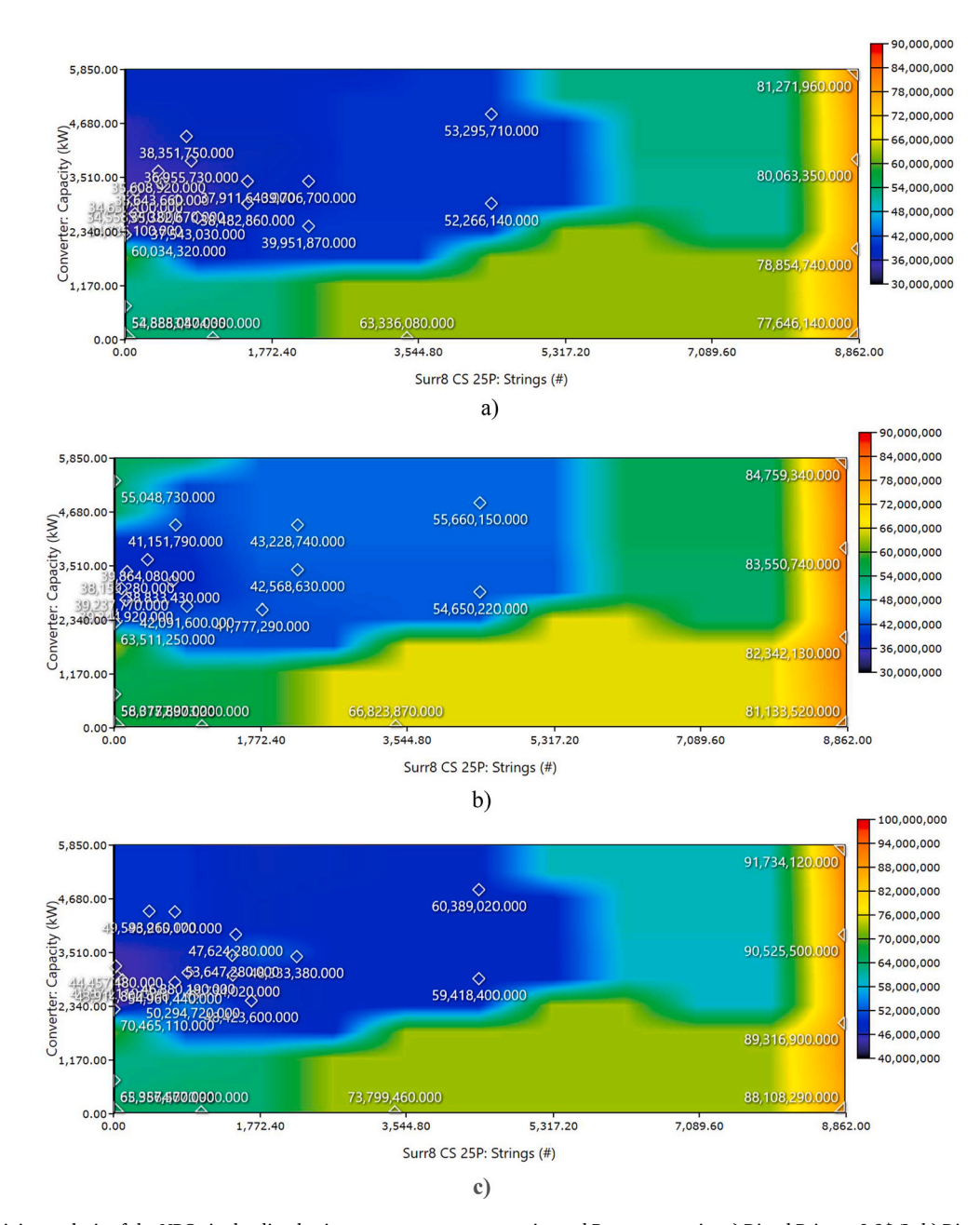


Fig. 17. The sensitivity analysis of the NPC via the diesel price among converter capacity and Battery capacity a) Diesel Price = 0.3\$/L, b) Diesel Price = 0.4\$/L and c) Diesel Price = 0.6\$/L.

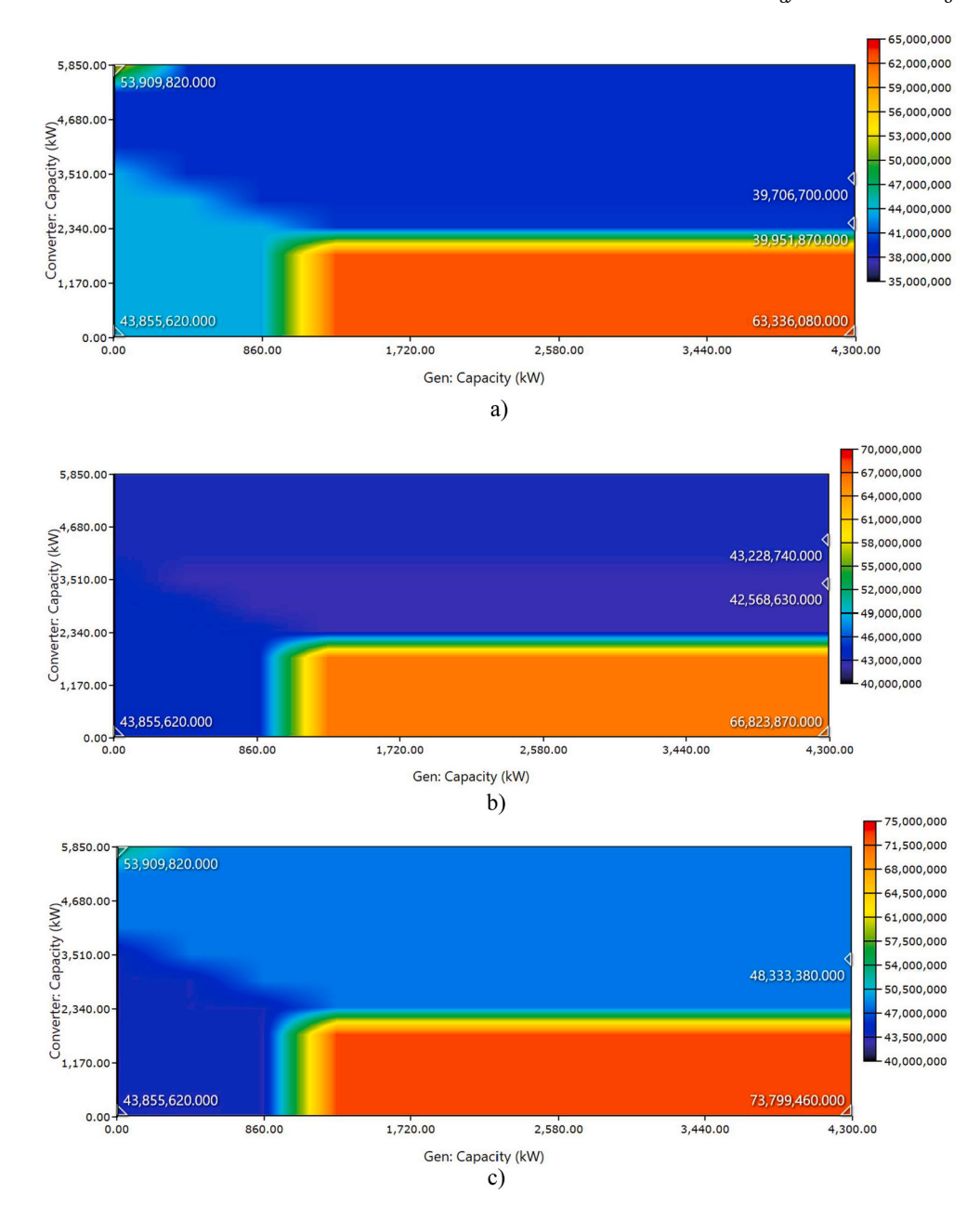


Fig. 18. The sensitivity analysis of the NPC via the diesel price among converter capacity and DG capacity, a) Diesel Price = 0.3\$/L, b) Diesel Price = 0.4\$/L and c) Diesel Price = 0.6\$/L.

capacity shortage increased sharply in under-optimized systems, while well-sized configurations maintained acceptable reliability. These results validate the importance of diesel price in microgrid economics. Optimizing storage and inverter capacity not only enhances technical performance but also mitigates financial risks associated with fuel cost fluctuations. For future deployments in fuel-volatile markets, systems with reduced generator dependence and robust renewable integration, particularly the MATLAB-linked configurations—offer superior long-term economic stability.

#### 6.8. Comparative analysis

A comparative analysis of the three strategies clearly indicates that the MATLAB-linked strategy outperforms both the CC and LF strategies in terms of economic and environmental metrics. The CC strategy, while providing stable power, incurs higher fuel consumption and operational costs due to the continuous operation of the diesel generator. The LF

strategy offers some improvements by making more effective use of renewable resources. However, neither strategy matches the performance of the MATLAB-linked approach, which maximizes renewable energy utilization and optimizes the operation of battery storage.

Table 13 shows that the HOMER Pro MATLAB Link Without DG achieves the highest renewable performance. It reaches 100 % in all key capacity and energy metrics. The Base System lacks renewable input. HOMER Cycle Charging and Load Following provide partial integration, with around 72 % nominal renewable capacity and 74–80 % renewable energy share. They meet their load with 99–103 % renewable generation and displace nonrenewables during peak output. The MATLAB Link With DG shows lower performance due to partial reliance on diesel. Overall, the MATLAB Link Without DG offers the most sustainable and efficient design.

Table 14 provides a detailed comparison of electricity generation, consumption, and system performance across the Base System and the three HOMER-optimized configurations: Cycle Charging, Load

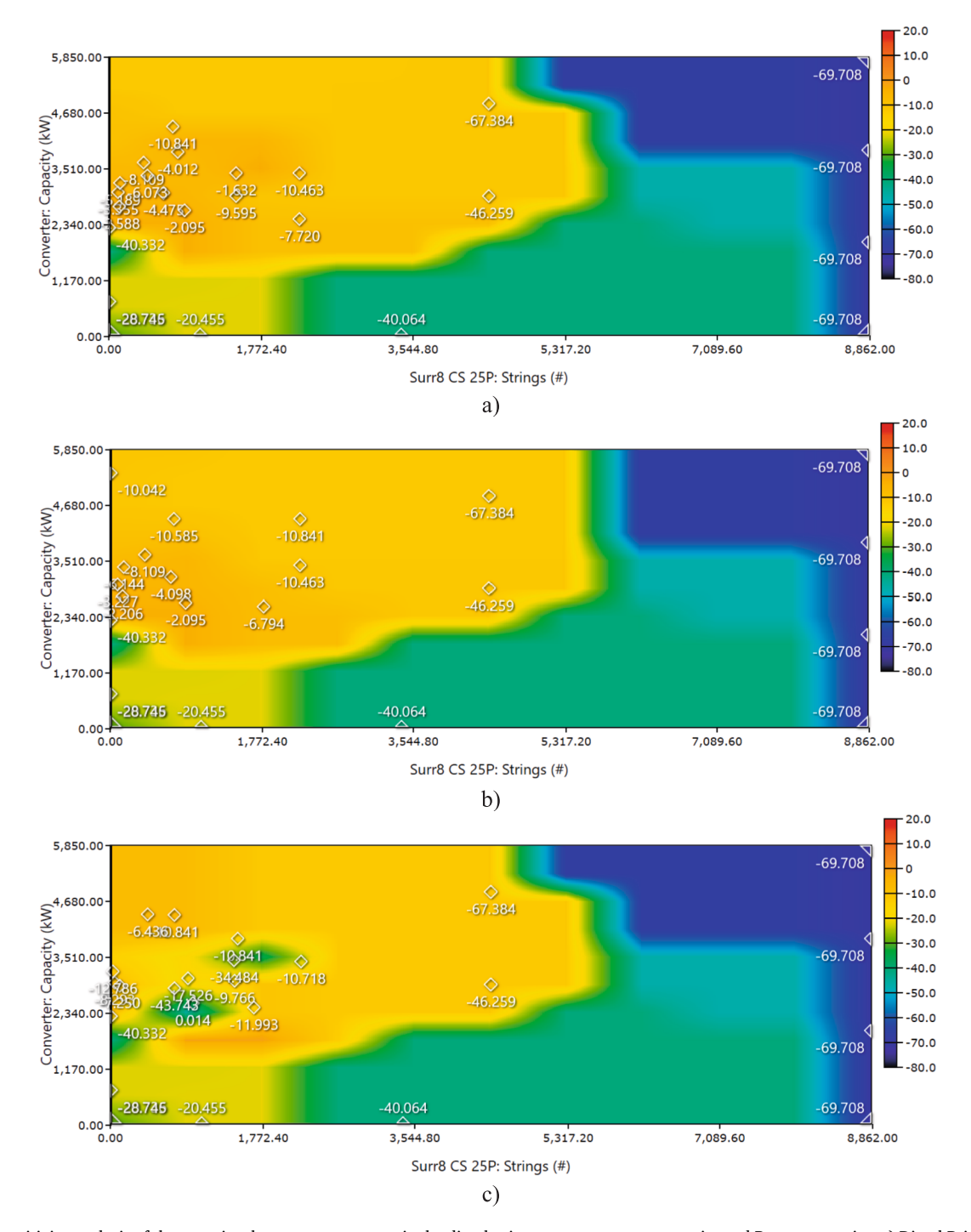


Fig. 19. The sensitivity analysis of the capacity shortage percentage via the diesel price among converter capacity and Battery capacity, a) Diesel Price = 0.4\$/L and c) Diesel Price = 0.6\$/L.

Following, and Pro MATLAB Link. The base system relies entirely on an autosized diesel genset, producing 18.5 million kWh/yr. It meets the full AC primary load of 18.4 million kWh/yr with no excess electricity, unmet load, or capacity shortage. No renewable sources are integrated, and the system does not include any DC or deferrable loads. The HOMER Cycle Charging integrates 10.6 million kWh/yr from PV (43 %) and 7.69 million kWh/yr from wind (31.2 %). The genset provides 6.38 million kWh/yr (25.9 %) to ensure load coverage. It generates 4.62 million kWh/yr of excess electricity with no unmet load or shortage. The full AC load is served reliably, indicating a successful balance between renewable inputs and diesel support. In the HOMER Load Following, PV

contributes 14.7 million kWh/yr (62.1 %), wind adds 4.31 million kWh/yr (18.2 %), and the genset generates 4.65 million kWh/yr (19.7 %). Excess electricity reaches 3.56 million kWh/yr. Like the Cycle Charging setup, it meets the entire AC primary load without any capacity shortage or unmet load. The system leans more on PV than wind or diesel, improving renewable utilization. The HOMER Pro MATLAB Link Without DG configuration operates on a fully renewable mix, with 27.4 million kWh/yr from PV (93.1 %) and 2.02 million kWh/yr from wind (6.87 %). No diesel generation is used. It produces the highest excess electricity at 12.2 million kWh/yr. However, it suffers from an unmet load of 9.44 million kWh/yr and a capacity shortage of 92,453 kWh/yr,

**Table 13**The analysis of the renewable energy performance across the designed configurations.

Capacity-based metrics	Unit	Base System	HOMER Cycle Charging	HOMER Load Following	HOMER Pro MATLAB Link	
					Without DG	With DG
Nominal renewable capacity divided by total nominal capacity	%	_	72.2	71.5	100	70.4
Usable renewable capacity divided by total capacity	%	_	50.6	58.7	100	51.0
Energy-based metrics						
Total renewable production divided by load	%	_	99.3	103	328	92.9
Total renewable production divided by generation	%	_	74.1	80.3	100	65.1
One minus total nonrenewable production divided by load	%	_	65.4	74.7	100	50.3
Peak values						
Renewable output divided by load (HOMER standard)	%	_	792	867	1,410	751
Renewable output divided by total generation	%	_	100	100	100	100
One minus nonrenewable output divided by total load	%	_	100	100	100	100

Table 14
The detailed comparison of electricity generation, consumption, and system performance across the designed configurations.

Quantity	Units	Base System		HOMER Cycle Charging		HOMER Load Following		HOMER Pro MATLAB Link without DG		HOMER Pro MATLAB Link with DG	
		Value	%	Value	%	Value	%	Value	%	Value	%
Excess Electricity	kWh/yr	114,640	_	4,622,829	_	3,560,446	_	12,202,519	_	6,131,851	
Unmet Electric Load	kWh/yr	0	_	0	_	0	_	9,442,893	_	0	_
Capacity Shortage	kWh/yr	0	_	0	_	0	_	92,453	_	0	_
PV	Production (kWh/yr)	0		10,604,283	43	14,712,215	62.1	27,416,318	93.1	10,765,474	41.0
Autosize Genset	Production (kWh/yr)	18,526,172	100	6,378,390	25.9	4,654,457	19.7	0		9,157,062	34.9
Eocycle EOX M-21 [100 kW]	Production (kWh/yr)	0	0	7,685,290	31.2	4,314,549	18.2	2,022,445	6.87	6,336,993	24.1
AC Primary Load	Consumption (kWh/yr)	18,411,531	100	18,411,531	100	18,411,531	100	8,968,639	100	18,418,297	100
DC Primary Load	Consumption (kWh/yr)	0	0	0	0	0	0	0	0	0	0
Deferrable Load	Consumption (kWh/yr)	0	0	0	0	0	0	0	0	0	0
Total	Consumption (kWh/yr)	18,411,531	100	18,411,531	100	18,411,531	100	8,968,639	100	18,418,297	100

managing to serve only 8.97 million kWh/yr of AC load. These results reflect the limitations of intermittent renewables without dispatchable backup. The HOMER Pro MATLAB Link With DG with genset support restored, this system generates 10.77 million kWh/yr from PV (41 %), 6.33 million kWh/yr from wind (24.1 %), and 9.16 million kWh/yr from the genset (34.9 %). Excess electricity drops to 6.13 million kWh/yr, and the system fully meets the AC load without any shortage or unmet demand. This hybrid setup improves reliability while still leveraging significant renewable input.

# 6.9. Limitations of HOMER pro MATLAB Link as strategy and excess load

The HOMER Pro MATLAB Link strategy is highly efficient in reducing reliance on non-renewable energy by leveraging advanced optimization techniques and maximizing renewable energy integration. However, despite its impressive performance, there are key limitations related to energy shortages and excess load that need to be addressed for this system to operate more reliably and sustainably.

# 6.9.1. Energy shortages

The HOMER Pro MATLAB Link strategy, with its 100 % reliance on renewable energy without DG, can face significant energy shortages during periods of low renewable generation. Renewable sources like solar PV and wind are intermittent by nature, meaning that when the sun is not shining or the wind is not blowing, the system may struggle to meet the energy demand. This challenge is exacerbated if the energy storage capacity is insufficient to buffer the fluctuations in renewable energy production. In the Pro MATLAB Link configuration, this can lead to unmet load, which reduces the reliability of the system.

# Factors contributing to energy shortages:

Intermittency of Renewable Resources: Solar and wind energy production are highly dependent on weather conditions and time of day,

leading to potential periods of low or no generation. Without adequate energy storage or backup systems, the microgrid may experience shortages.

- Limited Energy Storage: While the Pro MATLAB Link system may
  have some storage capacity, it might not be sufficient to cover prolonged periods of low renewable generation. Storage systems typically have limited autonomy (a few hours to a day), and if the storage
  is depleted, the system may not be able to meet the load demand.
- No Backup Generation: The HOMER Pro MATLAB Link strategy eliminates traditional backup generators, which are often used to prevent shortages during periods of low renewable production. Without backup generation, the system becomes vulnerable to supply shortfalls.
- Peak Demand Periods: During periods of high energy demand, especially if they coincide with low renewable generation, the system may not have enough capacity to meet the load. This can result in unmet load and disruptions to critical services.

#### Impact of shortages:

- Unmet Load: The unmet load in the HOMER Pro MATLAB Link system reflects instances where the system fails to supply sufficient energy to meet demand, potentially leading to service interruptions or reliance on external energy sources, which may increase costs.
- Decreased Reliability: Frequent shortages can reduce the overall reliability of the system, making it less suitable for critical applications where a consistent energy supply is crucial.

# 6.9.2. Excess electricity

While shortages are a concern, the HOMER Pro MATLAB Link system without DG may also experience significant periods of excess electricity production, where renewable energy generation exceeds the load demand. This is particularly common in systems with large renewable capacities, such as solar PV or wind farms, which can produce more

energy than needed during favorable conditions.

#### Factors contributing to excess electricity:

- Oversized Renewable Capacity: To compensate for the intermittency
  of renewables, microgrid systems are often designed with oversized
  renewable capacities. While this helps during periods of low generation, it can lead to excess electricity during periods of high renewable output.
- Limited Energy Storage Utilization: When storage systems reach full
  capacity, any additional renewable energy produced cannot be
  stored. Without effective utilization or export options, this excess
  electricity is wasted.
- Low Load Periods: During times of reduced energy consumption, such as overnight or during off-peak hours, the system may produce more electricity than is required. Without demand-response mechanisms or load-shifting strategies, this excess energy goes unused.

# Impact of excess electricity:

- Wasted Renewable Generation: Excess electricity that cannot be stored or used represents wasted potential energy. While renewable energy has low marginal costs, wasted energy still reflects a lost opportunity to optimize the system's efficiency and costeffectiveness.
- Underutilization of Resources: If the system frequently generates more energy than needed, this underutilization of resources could mean that capital investments in renewable energy and storage systems are not fully optimized, leading to inefficiencies.
- Higher LCOE: Wasted energy can drive up the LCOE by increasing the total system costs without a corresponding increase in usable energy output. This can make the system less financially viable over time.

#### 6.9.3. Potential solutions to address these limitations

- Improve Energy Storage Systems: Increasing storage capacity or incorporating more advanced energy storage technologies could help mitigate shortages by allowing excess renewable energy to be stored and used during periods of low generation. Improved energy storage would also help reduce the amount of excess electricity that is wasted.
- Demand-Side Management: Implementing demand-response strategies can help align energy consumption with periods of high renewable generation. For instance, scheduling non-critical loads or deferrable loads (e.g., water pumping, electric vehicle charging) to run during periods of excess electricity can help absorb surplus energy and prevent waste.
- 3. Backup Generation: While the goal of the HOMER Pro MATLAB Link strategy is to minimize or eliminate non-renewable energy sources, incorporating a small, efficient backup generator could help address energy shortages during critical periods. This would improve system reliability without heavily increasing the environmental impact.
- 4. Grid Interconnection: Connecting the microgrid to the main grid or other nearby microgrids can provide a mechanism for exporting excess electricity. This would help prevent energy waste while also creating a potential revenue stream through energy sales. Similarly, the grid connection can help supply energy during shortages, reducing unmet load.
- 5. Hybrid Energy Systems: Introducing additional renewable sources, such as small-scale hydropower or biomass, can help smooth out the variability in solar and wind production. By diversifying the energy mix, the system can reduce both excess electricity and shortages.
- Energy Efficiency and Load Shifting: Encouraging energy efficiency and load-shifting strategies within the microgrid can help better align energy consumption with production. This reduces the risk of

shortages during high-demand periods and prevents excess electricity during low-demand times.

While the HOMER Pro MATLAB Link strategy with DG excels in maximizing renewable energy integration, the limitations of energy shortages and excess electricity need to be addressed for optimal performance. Improving energy storage, incorporating demand-side management, and exploring grid interconnection or backup generation options can help mitigate these challenges. By addressing these limitations, the system can better balance energy production and consumption, improving reliability and overall system efficiency while reducing both unmet load and excess electricity.

#### 7. Conclusion

This paper evaluates the performance of various microgrid configurations, including the Base System, HOMER Cycle Charging, HOMER Load Following, and HOMER Pro MATLAB Link, with and without DG with a focus on renewable energy integration, energy storage, and system optimization for a case study of Sharoura, KSA. The results demonstrate that increasing renewable energy capacity and optimizing system operations can significantly reduce both costs and environmental impact. The Base System, which relies entirely on an autosized diesel generator, has the highest NPC of \$47.8 M and fuel consumption of 4.92 million liters per year. It produces 12.89 million kg of CO<sub>2</sub> emissions annually, highlighting its unsustainability in both financial and environmental terms. In contrast, the HOMER Cycle Charging system reduces fuel consumption by 67 % to 1.63 million liters per year and cuts CO<sub>2</sub> emissions by over 66 %, lowering the NPC to \$35.8 M. The HOMER Load Following configuration further reduces fuel consumption to 1.24 million liters and CO2 emissions to 3.26 million kg/yr, resulting in an NPC of \$33.7 M. The HOMER Pro MATLAB Link configuration achieves the lowest NPC of \$16.4 M by relying completely on renewable energy, eliminating fuel consumption and CO2 emissions. This configuration generates 328 % of the required load from renewable sources, resulting in 12.2 million kWh of excess electricity per year. However, it also faces challenges with unmet load, with approximately 9.44 million kWh/yr of demand not being met due to limitations in renewable energy availability and storage. Overall, the integration of renewable energy in the HOMER-optimized configurations leads to significant reductions in operational costs, fuel consumption, and emissions. However, these systems also face challenges, such as energy shortages during periods of low renewable production and excess electricity during peak generation. These findings highlight the need for careful system design, balancing renewable energy capacity with energy storage and load management to maximize reliability and cost-efficiency. Future work should focus on addressing the limitations related to energy shortages and excess electricity in fully renewable systems like the HOMER Pro MATLAB Link configuration. Future work on microgrid systems should focus on enhancing energy storage solutions, such as flow batteries and hydrogen storage, to better manage the variability of renewable generation, reducing unmet load during low production periods and maximizing the use of excess electricity. Demand-side management strategies, including load-shifting and smart demand-response, can help align energy consumption with periods of high renewable production, improving overall system efficiency. The introduction of hybrid energy systems, integrating additional renewable sources like hydropower or biomass, can provide more consistent energy generation, reducing reliance on intermittent sources and lowering the risk of shortages. Grid interconnection for energy export and import offers another avenue to mitigate shortages and excess electricity, creating opportunities for revenue generation and improving reliability. Moreover, the future work should also explore alternative storage options such as hydrogen, CAES, and pumped hydro. These technologies offer longer-duration storage and may enhance system reliability and flexibility. A comparative analysis will help evaluate their performance and cost-effectiveness. Lastly, optimizing renewable capacity through advanced forecasting tools and predictive algorithms will facilitate better balance energy supply and demand, minimizing both excess electricity and unmet load.

# CRediT authorship contribution statement

Saleh Awadh AL Dawsari: . Fatih Anayi: Writing – review & editing, Visualization, Supervision, Methodology, Investigation, Conceptualization. Michael Packianather: Supervision.

#### **Declaration of competing interest**

The authors declare that they have no known competing financial interests or personal relationships that could have appeared to influence the work reported in this paper.

#### Appendix A. Supplementary data

Supplementary data to this article can be found online at https://doi.org/10.1016/j.ecmx.2025.101386.

#### Data availability

The data that has been used is confidential.

#### References

- [1] Toopshekan A, Ahmadi E, Abedian A, Vaziri Rad MA. Techno-economic analysis, optimization, and dispatch strategy development for renewable energy systems equipped with Internet of Things technology. Energy 2024;296:131176. https://doi.org/10.1016/j.energy.2024.131176.
- [2] H. M. Sultan, A. A. Zaki Diab, O. N. Kuznetsov, Z. M. Ali, and O. Abdalla, "Evaluation of the impact of high penetration levels of PV power plants on the capacity, frequency and voltage stability of Egypt's unified grid," *Energies (Basel)*, vol. 12, no. 3, 2019, doi: 10.3390/en12030552.
- [3] Y. Yang, S. Xia, P. Huang, J. Qian, "Energy transition: Connotations, mechanisms and effects," 2024. doi: 10.1016/j.esr.2024.101320.
- [4] Y. Yang, S. Xia, X. Qian, "Geopolitics of the energy transition," Dili Xuebao/Acta Geograph Sin, vol. 77, no. 8, 2022, doi: 10.11821/dlxb202208014.
- [5] International Energy Agency (IEA), "Global Energy Review 2025," Mar. 2025. Accessed: Jun. 03, 2025. [Online]. Available: www.iea.org.
- [6] Nassar YF, et al. Assessing the viability of solar and wind energy technologies in semi-arid and arid regions: a case study of Libya's climatic conditions. Appl Solar Energy Feb. 2024;60(1):149–70. https://doi.org/10.3103/S0003701X24600218.
- [7] A. M. Soomar, A. Hakeem, M. Messaoudi, P. Musznicki, A. Iqbal, and S. Czapp, "Solar Photovoltaic Energy Optimization and Challenges," 2022. doi: 10.3389/ fenrg.2022.879985.
- [8] O. A. Al-Shahri et al., "Solar photovoltaic energy optimization methods, challenges and issues: A comprehensive review," 2021. doi: 10.1016/j.jclepro.2020.125465.
- [9] O. N. Kuznetsov, H. M. Sultan, R. I. Aljendy, A. A. Zaki Diab, "Economic feasibility analysis of PV/wind/diesel/battery isolated microgrid for rural electrification in South Egypt," in Proceedings of the 2019 IEEE Conference of Russian Young Researchers in Electrical and Electronic Engineering, ElConRus 2019, 2019. doi: 10.1109/EIConRus.2019.8656764.
- [10] A. A. Zaki Diab, H. M. Sultan, I. S. Mohamed, N. Kuznetsov Oleg, and T. D. Do, "Application of different optimization algorithms for optimal sizing of pv/wind/diesel/battery storage stand-alone hybrid microgrid," *IEEE Access*, vol. 7, 2019, doi: 10.1109/ACCESS.2019.2936656.
- [11] Hassan Q, et al. Saudi Arabia energy transition: Assessing the future of green hydrogen in climate change mitigation. Int J Hydrogen Energy 2024;55. https:// doi.org/10.1016/j.ijhydene.2023.11.117.
- [12] M. S. Emeara, A. F. AbdelGawad, E. H. Ahmed, "Hybrid Renewable Energy System for a Sustainable House-Power-Supply," J Adv Res Fluid Mechan Therm Sci, vol. 87, no. 1, 2021, doi: 10.37934/arfmts.87.1.91107.
- [13] A. Suman, Role of renewable energy technologies in climate change adaptation and mitigation: A brief review from Nepal, 2021. doi: 10.1016/j.rser.2021.111524.
- [14] T. Kara, A. D. Şahin, "Implications of Climate Change on Wind Energy Potential," 2023. doi: 10.3390/su152014822.
- [15] Hassan Q, Sameen AZ, Salman HM, Jaszczur M, Al-Hitmi M, Alghoul M. Energy futures and green hydrogen production: Is Saudi Arabia trend? Result Eng 2023;18. https://doi.org/10.1016/j.rineng.2023.101165.
- [16] A. Balabel et al., "Potential of solar hydrogen production by water electrolysis in the NEOM green city of Saudi Arabia," World J Adv Eng Technol Sci, vol. 8, no. 1, 2023, doi: 10.30574/wjaets.2023.8.1.0133.
- [17] Y. H. A. Amran, Y. H. M. Amran, R. Alyousef, H. Alabduljabbar, "Renewable and sustainable energy production in Saudi Arabia according to Saudi Vision 2030; Current status and future prospects," 2020. doi: 10.1016/j.jclepro.2019.119602.

- [18] Homer Energy, "HOMER Hybrid Renewable and Distributed Generation System Design Software." 2016.
- [19] S. Razfar, H. Ahmadi Danesh Ashtiani, A. Khoshgard, "Simulation of electrical energy supply required by maad koush pelletizing complex using renewable energy sources and simulation with homer energy software," Resul Eng, vol. 21, 2024, doi: 10.1016/j.rineng.2024.101845.
- [20] E. Y. Alhawsawi, H. M. D. Habbi, M. Hawsawi, M. A. Zohdy, "Optimal Design and Operation of Hybrid Renewable Energy Systems for Oakland University," *Energies (Basel)*, vol. 16, no. 15, 2023, doi: 10.3390/en16155830.
- [21] Suresh V, Muralidhar M, Kiranmayi R. Modelling and optimization of an off-grid hybrid renewable energy system for electrification in a rural areas. Energy Reports 2020;6. https://doi.org/10.1016/j.egyr.2020.01.013.
- [22] UU Republik Indonesia et al., "Penentuan Alternatif lokasi tempat pembuangan Akhir (TPA) Sampah di kabupaten Sidoarjo, Energies (Basel), vol. 15, no. 1, 2022.
- [23] H. Z. Al Garni, A. Abubakar Mas'ud, D. Wright, "Design and economic assessment of alternative renewable energy systems using capital cost projections: A case study for Saudi Arabia," Sustain Energy Technol Assessm, vol. 48, 2021, doi: 10.1016/j. seta.2021.101675.
- [24] S. Yadav, P. Kumar, A. Kumar, "Optimal Design of PV/WT/Battery Based Microgrid for Rural Areas in Leh Using Dragonfly Algorithm," Distribut Generat Alternative Energy J, pp. 221–262, Feb. 2024, doi: 10.13052/dgaej2156-3306.3922.
- [25] W. N. Adger, S. Fransen, R. S. de Campos, W. C. Clark, Migration and sustainable development, Proc Natl Acad Sci U S A, vol. 121, no. 3, 2024, doi: 10.1073/ pnas.2206193121.
- [26] F. Rohde et al., Broadening the perspective for sustainable artificial intelligence: sustainability criteria and indicators for Artificial Intelligence systems, 2024. doi: 10.1016/j.cosust.2023.101411.
- [27] M. Farghali et al., Social, environmental, and economic consequences of integrating renewable energies in the electricity sector: a review, 2023. doi: 10.1007/s10311-023-01587-1.
- [28] J. Martinez-Rico, E. Zulueta, I. R. De Argandona, U. Fernandez-Gamiz, M. Armendia, Multi-objective Optimization of Production Scheduling Using Particle Swarm Optimization Algorithm for Hybrid Renewable Power Plants with Battery Energy Storage System, J Mod Power Syst Clean Energy, vol. 9, no. 2, 2021, doi: 10.35833/MPCE.2019.000021.
- [29] M. A. Mquqwana, S. Krishnamurthy, "Particle Swarm Optimization for an Optimal Hybrid Renewable Energy Microgrid System under Uncertainty," Energies (Basel), vol. 17, no. 2, 2024, doi: 10.3390/en17020422.
- [30] P. Benalcazar, A. Suski, J. K. Nski, Optimal Sizing and Scheduling of Hybrid Energy Systems: The Cases of Morona Santiago and the Galapagos Islands, *Energies (Basel)*, vol. 13, no. 15, 2020, doi: 10.3390/en13153933.
- [31] Y. Sawle, S. C. Gupta, A. K. Bohre, Review of hybrid renewable energy systems with comparative analysis of off-grid hybrid system, 2018. doi: 10.1016/j. rser.2017.06.033.
- [32] C. Palanichamy, P. Naveen, Micro grid for All India Institute of Medical Sciences, Madurai, Clean Energy, vol. 5, no. 2, 2021, doi: 10.1093/ce/zkab007.
- [33] K. Karunanithi, S. P. Raja, S. Ramesh, K. Karthikumar, P. Chandrasekar, K. A. Rani, "Investigations on Off-Grid Hybrid Renewable Energy Microgrid for Sustainable Development Growth," *J Circuits, Syst Comput*, vol. 31, no. 6, 2022, doi: 10.1142/ S0218126622300033.
- [34] P. Hemim, P. S, "Challenges Hindering Electric Vehicle Adoption in India and Proposed Solutions," Qeios, 2024, doi: 10.32388/bt3xs1.
- [35] M. Gupta, A. Bhargava, Optimal design of hybrid renewable-energy microgrid system: a techno-economic-environment-social- reliability perspective, *Clean Energy*, vol. 8, no. 1, 2024, doi: 10.1093/ce/zkad069.
- Energy, vol. 8, no. 1, 2024, doi: 10.1093/ce/zkad069.

  [36] S. Sharma and Y. R. Sood, "Microgrids: A Review of Status, Technologies, Software Tools, and Issues in Indian Power Market," 2022. doi: 10.1080/02564602 2020 1850367
- [37] Yadav S, Kumar P, Kumar A. Optimal design and energy management in isolated renewable sources based microgrid considering excess energy and reliability aspects. J Energy Storage Dec. 2024;103:114320. https://doi.org/10.1016/j. est.2024.114320.
- [38] Abuhelwa M, Elnaggar M, Salah WA, Nassar YF, Bashir MJK. Exploring the prevalence of renewable energy practices and awareness levels in Palestine. Energy Sci Eng 2025;13(3):1292–305. https://doi.org/10.1002/ese3.2070.
- [39] A. F. M. Ali, E. M. H. Karram, Y. F. Nassar, A. A. Hafez, "Reliable and Economic Isolated Renewable Hybrid Power System with Pumped Hydropower Storage," in 2021 22nd International Middle East Power Systems Conference (MEPCON), IEEE, Dec. 2021, pp. 515–520. doi: 10.1109/MEPCON50283.2021.9686233.
- [40] Nassar YF, et al. Dynamic analysis and sizing optimization of a pumped hydroelectric storage-integrated hybrid PV/Wind system: a case study. Energy Convers Manag 2021;229:113744. https://doi.org/10.1016/j.
- [41] H. J. El-Khozondar, F. El-Batta, R. J. El-Khozondar, Y. Nassar, M. Alramlawi, S. Alsadi, Standalone hybrid PV/wind/diesel-electric generator system for a COVID-19 quarantine center, Environ Prog Sustain Energy, pp. e14049–e14049, Dec. 2022, doi: 10.1002/ep.14049.
- [42] Almihat MMG, Kahn MMTE. Design and implementation of Hybrid Renewable energy (PV/Wind/Diesel/Battery) Microgrids for rural areas. Solar Energy Sustain Dev J 2023;12(1):71–95. https://doi.org/10.51646/jsesd.v12i1.151.
- [43] L. Bilir, N. Yildirim, "Modeling and Performance Analysis of a Hybrid System for a Residential Application," in *Renewable Energy Sources*, University of Maribor Press, Jul. 2017, pp. 33–44. doi: 10.18690/978-961-286-061-5.4.
- [44] Nassar Y, Mangir I, Hafez A, El-Khozondar H, Salem M, Awad H. Feasibility of innovative topography-based hybrid renewable electrical power system: A case

- study. Clean Eng Technol 2023;14:100650. https://doi.org/10.1016/j.
- [45] Nassar YF, El-khozondar HJ, Ahmed AA, Alsharif A, Khaleel MM, El-Khozondar RJ. A new design for a built-in hybrid energy system, parabolic dish solar concentrator and bioenergy (PDSC/BG): A case study – Libya. J Clean Prod 2024;441:140944. https://doi.org/10.1016/j.jclepro.2024.140944.
- [46] Nassar YF, El-Khozondar HJ, Fakher MA. The role of hybrid renewable energy systems in covering power shortages in public electricity grid: An economic, environmental and technical optimization analysis. J Energy Storage 2025;108: 115224. https://doi.org/10.1016/j.est.2024.115224.
- [47] Nyasapoh MA, et al. Integrated Assessment of Nuclear-Renewable Hybrid Energy Systems: A Pathway to Sustainable and Resilient Industrial Electrification in Ghana. African J Appl Res 2025;11(2):22–46. https://doi.org/10.26437/ajar. v11i2.969.
- [48] Nyasapoh M, et al. Navigating renewable energy transition challenges for a sustainable energy future in Ghana. Solar Energy Sustain Dev J 2025;14(1): 237–57. https://doi.org/10.51646/jsesd.v14i1.479.
- [49] Z. Serat, M. Danishmal, F. Mohammad Mohammadi, Optimizing hybrid PV/Wind and grid systems for sustainable energy solutions at the university campus: Economic, environmental, and sensitivity analysis, Energy Convers Manage: X, vol. 24, p. 100691, Oct. 2024, doi: 10.1016/j.ecmx.2024.100691.
- [50] Hu P, Qian L, Li Z, Yu Y, Wang D. Distributed dynamic economic dispatch of biogas-wind-solar-hydrogen multi-microgrid system considering individual selfishness. Energy Convers Manage: X Oct. 2024;24:100761. https://doi.org/ 10.1016/j.ecmx.2024.100761.
- [51] Md. F. Ali, Md. R. Islam Sheikh, M. Md. Julhash, and A. H. Sanvi, "Sustainable electrification of remote communities: Techno-economic and demand response analysis for renewable microgrids," *Energy Convers Manage: X*, vol. 26, p. 100963, Apr. 2025, doi: 10.1016/j.ecmx.2025.100963.
- [52] A. A. A. Aqila, Y. Nassar, H. El-Khozondar, "Determining the Least Risky Solar Radiation Transposition Model for Estimating Global Inclined Solar Irradiation," Solar Energy Sustain Dev J, vol. 14, no. FICTS-2024, pp. 1–16, Jan. 2025, doi: 10.51646/isesd.v14iFICTS-2024.440.
- [53] S. Ba-swaimi, R. Verayiah, V. K. Ramachandaramurthy, A. K. ALAhmad, and A. Abu-Rayash, "Development and techno-economic assessment of an optimized and integrated solar/wind energy system for remote health applications," *Energy Convers Manage: X*, vol. 26, p. 100985, Apr. 2025, doi: 10.1016/j. ecmx.2025.100985.
- [54] Suganthi D, Jamuna K. Optimizing campus microgrid energy systems: economic, environmental, and sensitivity insights. Energy Convers Manage: X Jul. 2025;27: 101046. https://doi.org/10.1016/j.ecmx.2025.101046.
- [55] Y. W. Koholé, C. A. Wankouo Ngouleu, F. C. V. Fohagui, G. Tchuen, "Optimization and comparative analysis of hybrid renewable energy systems for sustainable and clean energy production in rural Cameroon considering the loss of power supply probability concept," *Energy Convers Manage: X*, vol. 25, p. 100829, Jan. 2025, doi: 10.1016/j.ecmx.2024.100829.
- [56] Kumar D. Urban energy system management for enhanced energy potential for upcoming smart cities. Energy Explorat Exploitat Sep. 2020;38(5):1968–82. https://doi.org/10.1177/0144598720937529.
- [57] Hong YY, Magararu LAP. Techno-economic analysis of Taiwan's new energy policy for 2025. Sustain Energy Technol Assessm Aug. 2021;46. https://doi.org/10.1016/ i.seta.2021.101307.
- [58] Das BK, Hasan M. Optimal sizing of a stand-alone hybrid system for electric and thermal loads using excess energy and waste heat. Energy Jan. 2021;214. https:// doi.org/10.1016/j.energy.2020.119036.
- [59] Ramesh M, Saini RP. Dispatch strategies based performance analysis of a hybrid renewable energy system for a remote rural area in India. J Clean Prod Jun. 2020; 259. https://doi.org/10.1016/j.jclepro.2020.120697.
- [60] A. Azahra, K. D. Syahindra, D. R. Aryani, F. H. Jufri, I. M. Ardita, "Optimized configuration of photovoltaic and battery energy storage system (BESS) in an isolated grid: A case study of Eastern Indonesia," in IOP Conference Series: Earth and Environmental Science, IOP Publishing Ltd, Nov. 2020. doi: 10.1088/1755-1315/599/1/012017.
- [61] H. Sharma and S. Mishra, "Hybrid Optimization Model for Smart Grid Distributed Generation Using HOMER".
- [62] S. Polat and Hacer Sekerci, "The Determination of Optimal Operating Condition For an Off-Grid Hybrid Renewable Energy Based Micro-Grid: a Case Study in Izmir, Turkey," EMITTER Int J Eng Technol, vol. 9, no. 1, pp. 137–153, Jun. 2021, doi: 10.24003/emitter.v9i1.597.
- [63] C. Malanda, A. B. Makokha, C. Nzila, C. Zalengera, "Techno-economic optimization of hybrid renewable electrification systems for Malawi's rural villages," *Cogent Eng*, vol. 8, no. 1, 2021, doi: 10.1080/23311916.2021.1910112.
- [64] Kumar A, Singh AR, Deng Y, He X, Kumar P, Bansal RC. Multiyear load growth based techno-financial evaluation of a microgrid for an academic institution. IEEE Access Jun. 2018;6:37533–55. https://doi.org/10.1109/ACCESS.2018.2849411.
- [65] T. F. Fofang, E. Tanyi, Design and Simulation of Off-Grid Solar/Mini-Hydro Renewable Energy System using Homer Pro Software: Case of Muyuka Rural Community. [Online]. Available: www.ijert.org.
- [66] Rezk H, Al-Dhaifallah M, Hassan YB, Ziedan HA. Optimization and Energy Management of Hybrid Photovoltaic-Diesel-Battery System to Pump and Desalinate Water at Isolated Regions. IEEE Access 2020;8:102512–29. https://doi.org/ 10.1109/ACCESS.2020.2998720.
- [67] Mubaarak S, et al. Potential techno-economic feasibility of hybrid energy systems for electrifying various consumers in Yemen. Sustainability (Switzerland) Jan. 2021;13(1):1–24. https://doi.org/10.3390/su13010228.

- [68] B. K. Das et al., "Optimum Design of a Grid Connected PV/Battery Hybrid System for Commercial Load in Bangladesh: Effects of PV, Battery, and Dispatch Strategies." [Online]. Available: https://www.researchgate.net/publication/ 348634245.
- [69] Z. Javid, K. J. Li, R. Ul Hassan, J. Chen, "Hybrid-microgrid planning, sizing and optimization for an industrial demand in Pakistan," *Tehnicki Vjesnik*, vol. 27, no. 3, pp. 781–792, Jun. 2020, doi: 10.17559/TV-20181219042529.
- [70] Soon KY, Chua KH, Lim YS, Wang L. A comprehensive methodology for setting up rural electrifications with minimum budgets on indigenous villages in Malaysia. Int J Energy Sector Manage Sep. 2019;13(4):885–902. https://doi.org/10.1108/ LIFSM-02-2018-0010.
- [71] Popoola OT, Rabiu AB, Ibrahim HK, Ajao KR, Bamigboye JT, Idakwoji IT, "Optimization of Photovoltaic-Wind Hybrid System for Electrifying University of Ilorin E-Library," 2021.
- [72] Yadav S, Kumar P, Kumar A. Techno-economic assessment of hybrid renewable energy system with multi energy storage system using HOMER. Energy Jun. 2024; 297:131231. https://doi.org/10.1016/j.energy.2024.131231.
- [73] Yadav S, Kumar P, Kumar A. Hybrid renewable energy systems design and technoeconomic analysis for isolated rural microgrid using HOMER. Energy Jul. 2025; 327:136442. https://doi.org/10.1016/j.energy.2025.136442.
- [74] S. Yadav, P. Kumar, and A. Kumar, "Techno-Economic and Sensitivity Analysis of Standalone Hybrid Energy System Using HOMER Software: A Case Study of Kanur Village in India," 2024, pp. 271–287. doi: 10.1007/978-981-99-7630-0 21.
- [75] Aziz AS, Tajuddin MFN, Zidane TEK, Su CL, Alrubaie AJK, Alwazzan MJ. Technoeconomic and environmental evaluation of PV/diesel/battery hybrid energy system using improved dispatch strategy. Energy Reports Nov. 2022;8:6794–814. https://doi.org/10.1016/j.egyr.2022.05.021.
- [76] "Solar resource map © 2021 Solargis." Accessed: Jun. 03, 2025. [Online]. Available: https://solargis.com.
- [77] Rehman S, Baseer MA, Alhems LM. GIS-based multi-criteria wind farm site selection methodology. FME Transactions 2020;48(4):855–67. https://doi.org/ 10.5937/fme2004855R.
- [78] Thirunavukkarasu M, Sawle Y. A Comparative Study of the Optimal Sizing and Management of Off-Grid Solar/Wind/Diesel and Battery Energy Systems for Remote Areas. Front Energy Res Nov. 2021;9. https://doi.org/10.3389/ fenrg.2021.752043.
- [79] Baruah A, Basu M, Amuley D. Modeling of an autonomous hybrid renewable energy system for electrification of a township: a case study for Sikkim, India. Renew Sustain Energy Rev Jan. 2021;135:110158. https://doi.org/10.1016/j. rser.2020.110158.
- [80] Olatomiwa L, Mekhilef S, Huda ASN, Sanusi K. Techno-economic analysis of hybrid PV-diesel-battery and PV-wind-diesel-battery power systems for mobile BTS: the way forward for rural development. Energy Sci Eng Jul. 2015;3(4):271–85. https://doi.org/10.1002/ese3.71.
- [81] Y. F. Nassar, S. Y. Alsadi, G. M. Miskeen, H. J. El-Khozondar, and N. M. Abuhamoud, "Mapping of PV Solar Module Technologies Across Libyan Territory," in 2022 Iraqi International Conference on Communication and Information Technologies (IICCIT), IEEE, Sep. 2022, pp. 227–232. doi: 10.1109/IICCIT55816.2022.10010476.
- [82] Nassar YF, et al. Carbon footprint and energy life cycle assessment of wind energy industry in Libya. Energy Convers Manag Jan. 2024;300:117846. https://doi.org/ 10.1016/j.enconman.2023.117846.
- [83] M. El Zein and G. Gebresenbet, "Investigating off-grid systems for a mobile automated milking facility," *Heliyon*, vol. 7, no. 4, 2021, doi: 10.1016/j. heliyon 2021 e06630
- [84] Hafez AA, Nassar YF, Hammdan MI, Alsadi SY. Technical and Economic Feasibility of Utility-Scale Solar Energy Conversion Systems in Saudi Arabia. Iran J Sci Technol, Trans Electr Eng Mar. 2020;44(1):213–25. https://doi.org/10.1007/ s40998-019-00233-3.
- [85] M. A. Tolba, A. A. Zaki Diab, A. S. Vanin, V. N. Tulsky, A. Y. Abdelaziz, "Integration of Renewable Distributed Generation in Distribution Networks Including a Practical Case Study Based on a Hybrid PSOGSA Optimization Algorithm," *Electric Power Compon Syst*, vol. 46, no. 19–20, 2018, doi: 10.1080/ 15325008.2018.1532470.
- [86] M. Salem, A. Elmabruk, M. Irhouma, and I. Mangir, "Assessment of Wind Energy Potential in Western Mountain: Nalut and Yefren as Case Study," Wadi Alshatti University J Pur Appl Sci, pp. 35–42, Mar. 2025, doi: 10.63318/waujpasv3i1\_7.
- [87] Elmariami A, El-Osta W, Nassar Y, Khalifa Y, Elfleet M. Life Cycle Assessment of 20 MW Wind Farm in Libya. Appl Solar Energy Feb. 2023;59(1):64–78. https://doi. org/10.3103/S0003701X22601557.
- [88] F. S. Mahmoud, A. M. Abdelhamid, A. Al Sumaiti, A. H. M. El-Sayed, and A. A. Z. Diab, "Sizing and Design of a PV-Wind-Fuel Cell Storage System Integrated into a Grid Considering the Uncertainty of Load Demand Using the Marine Predators Algorithm," *Mathematics*, vol. 10, no. 19, 2022, doi: 10.3390/math10193708.
- [89] Bhimaraju A, Bhanu Ganesh G, Mahesh A. Optimal Sizing of PV/Wind/Battery Grid-Connected Hybrid Renewable Energy Systems Using TLBO Algorithm. In: in Lecture Notes in Electrical Engineering; 2024. https://doi.org/10.1007/978-981-99-0235-5-2
- [90] Y. F. Nassar, H. J. El-Khozondar, S. Y. Alsadi, N. M. Abuhamoud, and G. M. Miskeen, "Atlas of PV Solar Systems Across Libyan Territory," in 2022 International Conference on Engineering & MIS (ICEMIS), IEEE, Jul. 2022, pp. 1–6. doi: 10.1109/ICEMIS56295.2022.9914355.
- [91] Abdunnabi M, Etiab N, Nassar YF, El-Khozondar HJ, Khargotra R. Energy savings strategy for the residential sector in Libya and its impacts on the global environment and the nation economy. Adv Build Energy Res Jul. 2023;17(4): 379–411. https://doi.org/10.1080/17512549.2023.2209094.

- [92] Eteriki MA, El-Osta WA, Nassar YF, Khozondar H-J-E. Effect of Implementation of Energy Efficiency in Residential Sector in Libya. In: in 2023 8th International Engineering Conference on Renewable Energy & Sustainability (ieCRES), IEEE; May 2023. p. 1–6. https://doi.org/10.1109/ieCRES57315.2023.10209521.
- 2023. p. 1–6. https://doi.org/10.1109/ieCRES57315.2023.10209521.

  [93] K. M. Anwarul Islam, "The Renewable Energy and Sustainable Development: A Case Study of Bangladesh," *Int J Finance Banking Res*, vol. 2, no. 4, 2016, doi: 10.11648/j.ijfbr.20160204.13.
- [94] S. W. Chisale, S. Eliya, and J. Taulo, "Optimization and design of hybrid power system using HOMER pro and integrated CRITIC-PROMETHEE II approaches," *Green Technol Sustainab*, vol. 1, no. 1, 2023, doi: 10.1016/j.grets.2022.100005.
- [95] A. M. Rehmani, S. A. A. Kazmi, A. Altamimi, Z. A. Khan, M. Awais, "Techno-Economic-Environmental Assessment of an Isolated Rural Micro-Grid from a Mid-Career Repowering Perspective," Sustainability (Switzerland), vol. 15, no. 3, 2023, doi: 10.3390/su15032137.
- [96] F. H. Jufri, D. R. Aryani, I. Garniwa, and B. Sudiarto, "Optimal battery energy storage dispatch strategy for small-scale isolated hybrid renewable energy system with different load profile patterns," *Energies (Basel)*, vol. 14, no. 11, 2021, doi: 10.3390/en14113139.